Maritime Chokepoint Disruptions, Trade, and U.S. Inflation*

Ricardo Reyes-Heroles† Xiaoqing Zhou‡

October 31, 2026

Abstract

We study the effects of maritime chokepoint disruptions on U.S. inflation and their implications for monetary policy. Using satellite tracking of vessels passing through the world's major chokepoints, we measure disruptions as the reallocation of shipping across the global maritime network. Because chokepoint disruptions originate in geopolitical conflicts, natural disasters, and accidents, they identify shipping shocks in a structural VAR. A disruption on the scale of a major chokepoint event raises U.S. consumer prices by about 0.2 percent for nearly two years, mostly through core prices, with transmission running from freight rates to import and producer prices. A quantitative multi-country general equilibrium model with nominal rigidities, in which disruptions raise the cost of trading goods across borders, reproduces these responses. We use the model to assess the 2023 Red Sea Crisis and the 2026 closure of the Strait of Hormuz, and to compare a policy rule that responds to consumer price inflation with rules that respond to producer price inflation or look through the disruption.

Keywords: Maritime Chokepoints; Shipping Disruptions; Supply Chain; Inflation; Trade Costs; Monetary Policy; Structural VAR; AIS Data.

JEL Codes: E31, E32, E52, F14, F41, R41.

*We thank David Berger, Loukas Karabarbounis, Lutz Kilian, Fernando Leibovici and Kei-Mu Yi for helpful comments and discussions. Timothy Fong provided excellent research assistance. The views in this paper are solely the responsibility of the authors and should not be interpreted as reflecting the views of the Federal Reserve Bank of Dallas or the Federal Reserve System.

†Federal Reserve Bank of Dallas. Email: ricardo.reyes-heroles@dal.frb.org

‡Federal Reserve Bank of Dallas. Email: xiaoqing.zhou@dal.frb.org

1 Introduction

More than 80 percent of world merchandise trade by volume travels by sea, and much of it transits through a handful of narrow passages such as the Suez and Panama Canals, the Bab el-Mandeb Strait, and the Strait of Hormuz. In recent years, these chokepoints have become a recurring source of disruption. In 2023, for example, drought reduced the number of ships that could transit the Panama Canal. Later that year, attacks on merchant vessels in the Red Sea pushed carriers onto a far longer route around the Cape of Good Hope. In 2026, military escalation in the Middle East brought shipping through the Strait of Hormuz to a near halt. Each episode raised the same questions for policymakers: How much of the inflation that followed was caused by the disruption? How long would it last? Should monetary policy respond, or look through it? The answers are not obvious. Shipping disruptions resemble trade policy shocks, energy price shocks, and the pandemic-era supply chain crisis, yet they are none of these, and their effects have been hard to separate from the shocks that tend to accompany them.

This paper answers these questions by combining new empirical evidence with a quantitative model of the world economy. We make three contributions. First, we build a monthly measure of maritime chokepoint disruptions from satellite tracking of vessel traffic through major chokepoints worldwide. Second, using this measure in a structural vector autoregression (SVAR) model, we show that shipping disruptions are a supply shock in their own right, with much of the inflationary effect running through core rather than energy and food prices. Third, we develop a multi-country trade model with nominal rigidities, in which shipping disruptions raise the cost of trading both intermediate and final goods across borders. Disciplined by our empirical estimates, the model reproduces the price and interest-rate responses in the data and traces the transmission of maritime disruptions to trade and output. We then use it to study the two largest chokepoint closures in recent years—the 2023 Red Sea Crisis and the 2026 closure of the Strait of Hormuz—and ask whether a central bank that targeted an alternative price index or looked through the rise in consumer prices would have done better.

The key empirical challenge is to measure maritime chokepoint disruptions in a way that is comparable across events and distinct from shipping prices themselves. Shipping prices are useful indicators of market stress, but they are equilibrium outcomes that reflect both supply and demand conditions. Broad supply chain indexes summarize many frictions but do not isolate the maritime component. We instead begin with physical vessel movements through the narrow passages that carry much of the world's seaborne trade. By measuring changes in the flow of ships across these corridors, we capture disruptions at the source, before they are reflected in prices.

Our data are satellite-based vessel-tracking records compiled by the IMF's PortWatch, which

give daily cargo volumes through 28 major chokepoints worldwide, separately for container ships, dry-bulk carriers, and tankers.[1] Two facts revealed by these data shape our measurement. First, disruptions are broad-based. The Red Sea Crisis, for instance, usually seen as a container shipping event, also pulled bulk and tanker traffic away from the Suez Canal. Second, disruptions are network events. Cargo that cannot pass one chokepoint reappears elsewhere, as ships reroute or buyers turn to suppliers on other routes. We therefore measure a disruption as a reallocation of traffic across the maritime network—the total shift in chokepoints' shares of shipping volume relative to a base year—motivated by the labor economics literature on sectoral reallocation. Since our measure is built from shares, it is insulated from swings in the overall volume of world trade.

While measuring disruptions at the source addresses part of the identification problem, what remains is to isolate movements in the measure that are exogenous to the U.S. economy. Here the causes of chokepoint disruptions help: geopolitical events, natural disasters, and vessel accidents lie outside the U.S. economy. We therefore exploit this in a structural VAR in which innovations to our measure are predetermined within the month with respect to U.S. consumer prices, interest rates, and energy prices. This assumption keeps energy market shocks from contaminating the shipping shock, while letting energy prices, inflation, and policy rates respond freely to the disruption. Furthermore, because shipping prices never enter the disruption measure, they become an outcome we can study rather than an input that clouds identification.

Our main empirical finding is that disruptions in distant waterways impact U.S. inflation and trigger monetary policy responses. A disruption of two standard deviations (about the scale of a major chokepoint event in the data) raises the PCE price level by about 0.2 percent at its peak, ten months after impact. The effect remains credibly positive for nearly two years. Much of the increase shows up in core prices. Tracing the shock through the economy reveals a chain of transmission. Global cargo volumes fall while freight rates jump, U.S. import prices rise for about a year, U.S. producer prices peak within seven months, and U.S. consumer prices follow. Short-term rates rise with a lag, consistent with monetary policy leaning against the inflationary pressure. Maritime shipping disruptions are therefore a supply shock in their own right, persistent enough to move core inflation and large enough to draw a policy response. These findings hold when we measure disruptions using container traffic alone and when we exclude the largest episodes in our sample.

The evidence above quantifies the effects of maritime chokepoint disruptions on prices and short-term interest rates, but it leaves open three important questions. Why do these disruptions

[1] Bai et al. (2026a) and Bai et al. (2026b) also use satellite-based data (AIS) to measure the effective capacity of the U.S.-bound container fleet and congestion at major container ports, respectively. Both measures capture conditions at the destination end of a voyage and are dominated by the pandemic-era surge in goods demand. Our measure records disruptions at the chokepoint where they occur, covers all freight categories, and differs from port congestion measures (see Section 2.3). We discuss the relation to these papers in more detail below.

generate persistent inflationary pressure, and how does that pressure propagate through the economy? What are the consequences for economic activity and international trade? To what extent does the monetary policy response shape these outcomes? To address these questions, we adapt the multi-country general equilibrium model of Cuba-Borda et al. (2025), which is designed to quantify the macroeconomic effects of bilateral trade disruptions and their propagation through the global economy. Chokepoint disruptions enter the model as increases in the cost of trading goods across borders.[2]

The model separates the immediate effect of shipping disruptions on the cost of imported goods from their broader consequences for domestic production and prices. Because it distinguishes imports of final goods from imports of intermediate inputs, higher shipping costs raise both the prices consumers pay for imports on impact and the cost of imported inputs for firms, and hence firms' real marginal costs. With nominal rigidities, firms respond by raising producer prices and reducing production over time, so that the disruption behaves like an adverse domestic supply shock with persistent effects on inflation and output.[3] As these effects unfold, each country's central bank responds according to its own policy rule, and these responses shape equilibrium inflation and economic activity, while international goods and financial markets adjust through exchange rates and trade flows. The consequences of a shipping disruption thus extend beyond the prices of imported goods to domestic production, aggregate demand, and the external accounts.

We take the model to the data in two steps. First, we calibrate the model and construct a trade cost shock whose effect on shipping costs matches the estimated response of freight rates to an average maritime chokepoint disruption. Because the model includes more than two countries and route-specific trade costs, we compute the effect of a disruption to each U.S. trading route and average across routes, which yields a model counterpart to the average disruption identified in the data. Second, we compare the model's responses of U.S. prices and interest rates to this shock with the SVAR estimates. Since the calibration does not target these responses, the comparison provides an independent check on the model.

The model performs well in this comparison. A disruption that raises trade costs by 12 percent, the increase corresponding to a two-standard-deviation rise in our disruption measure, generates increases in U.S. consumer and producer prices and a rise in short-term interest rates that are broadly consistent with the SVAR evidence. The model also predicts a persistent contraction in

[2] Dunn and Leibovici (2023) and Bai et al. (2026a) study shipping disruptions in real quantitative models. Our work complements theirs by introducing nominal rigidities and country-specific monetary policy, which allows us to study the inflationary effects of shipping disruptions and the policy response to them.

[3] Gilchrist et al. (2026) provide evidence using firm-level data that higher shipping costs lead to persistent increases in U.S. producer prices, especially during the COVID-19 pandemic. Our evidence and model mechanisms complement their empirical and theoretical work, respectively.

economic activity: U.S. GDP falls by about 0.4 percent after four quarters, and imports and exports decline substantially. These effects arise primarily because higher shipping costs raise the cost of intermediate inputs. The model thus provides a unified account of how physical disruptions to maritime transportation raise inflation, depress output, and reduce cross-border trade.

Finally, we use the model to quantify the macroeconomic effects of the two largest chokepoint disruptions in our sample, the Red Sea Crisis that began in late 2023 and the closure of the Strait of Hormuz in March 2026, and the role of monetary policy in shaping them. For each episode, we calibrate route-specific increases in shipping costs to the data and compare outcomes under the baseline monetary policy rule, which responds to consumer price inflation, and two alternative counterfactual rules: one in which the Federal Reserve responds to producer price inflation instead, and one in which it holds the policy rate unchanged. The counterfactuals capture policies that look through, partially or completely, the increase in consumer prices caused by a supply disruption.

We find that the Red Sea Crisis added about 0.4 percentage point to U.S. consumer price (PCE) inflation by the end of 2024 and lowered GDP by about 1.1 percent, with small movements in the real exchange rate and the trade balance. Targeting producer price (PPI) inflation would have changed little, because producer prices reflect the rise in firms' marginal costs from higher prices of imported inputs and therefore move together with consumer prices. Holding the policy rate unchanged would have raised the inflation cost to about 0.6 percentage point while limiting the decline in GDP to 0.2 percent. The closure of the Strait of Hormuz had smaller effects through the shipping channel alone, setting aside its effect on energy prices. It added about 0.2 percentage point to PCE inflation and lowered GDP by about 0.6 percent by late 2026, but its effect on prices was more persistent, because the disruption fell mainly on goods that consumers do not buy directly. These results illustrate the trade-off a central bank faces following a maritime shipping disruption: a more accommodative policy moderates the short-run decline in output but does not eliminate the inflationary effect of higher trade costs, and it need not deliver a uniformly better macroeconomic adjustment.

Relation to the Literature. Our paper contributes to three strands of literature: the empirical work on shipping and supply chain disruptions and inflation, quantitative models of trade costs, and the design of monetary policy in response to supply shocks. Within the first, one branch develops measures of supply chain disruptions. Benigno et al. (2022) construct the Global Supply Chain Pressure Index by combining transportation-cost measures with survey-based indicators of delivery times and supply chain conditions, and Burriel et al. (2024) build a bottleneck index from newspaper text. Känzig and Raghavan (2026) focus specifically on maritime disruptions, using narrative accounts of disruptions at two chokepoints—the Suez and Panama Canals—with high-frequency movements in freight rates to identify supply chain shocks. Bai et al. (2026b)

instead use satellite-based vessel-tracking data on container ships to measure congestion at major ports around the world, while Bai et al. (2026a) use these data to measure effective shipping capacity along U.S.-bound container routes.

A second branch estimates the inflationary effects of these disruptions. Carrière-Swallow et al. (2023) and Isaacson and Rubinton (2023) document that increases in shipping costs pass through to consumer and import prices; Finck and Tillmann (2023), Ascari et al. (2024), and Finck et al. (2026) identify supply chain shocks in structural VARs; and di Giovanni et al. (2022) and Comin et al. (2023) quantify the contribution of supply chain constraints to the post-pandemic inflation. Our approach differs in measuring physical disruptions in maritime shipping across the global network of chokepoints. This allows us to treat freight rates as endogenous market outcomes rather than as inputs into the disruption measure, and to trace the transmission of physical shipping disruptions through freight rates, energy and import prices, and ultimately U.S. inflation.

Our quantitative analysis relates to the literature on the macroeconomic effects of disruptions in international trade linkages. We build on the multi-country framework of Cuba-Borda et al. (2025), which suits our analysis for two main reasons. First, in contrast to the recent literature on tariff shocks and monetary policy (Auray et al., 2025; Auclert et al., 2025; Monacelli, 2025; Schmitt-Grohé and Uribe, 2026; Bianchi and Coulibaly, 2025; Werning et al., 2025), the framework allows for shocks to broadly defined trade costs, including shipping disruptions across multiple trade routes. Second, relative to recent models of shipping disruptions (Dunn and Leibovici, 2023; Bai et al., 2026b; Gilchrist et al., 2026), it incorporates sluggish price adjustment and monetary policy in a global economy, which allows us to study the short-run dynamics of prices and output following a disruption.[4] We adapt this framework to maritime chokepoint disruptions, discipline the trade cost shocks with our empirical estimates, and examine their implications for prices, output, and international trade.

Our counterfactual analysis contributes to the literature on the design of monetary policy in response to supply shocks in open economies, which has recently focused on tariffs (Bergin and Corsetti, 2023; Bianchi and Coulibaly, 2025; Bodenstein et al., 2026). We contribute by examining a different source of trade costs, and the distinction matters: shipping disruptions are technological rather than policy shocks. To our knowledge, this is the first paper to quantify the role of monetary policy in response to shipping disruptions.

Outline. The paper proceeds as follows. Section 2 provides background on maritime chokepoints,

[4] An exception is Bai et al. (2026c), who study monetary policy in response to global supply chain disruptions. Their analysis differs from ours in relying on a stylized model to discipline the empirical analysis rather than developing a quantitative framework, which is what allows us to assess the size of the effects of specific disruptions and to compare outcomes under alternative monetary policy rules.

describes the data, develops our measure of maritime chokepoint disruptions, and compares it with alternative measures of supply chain conditions. Section 3 uses a structural VAR to estimate the effects of maritime chokepoint disruption shocks on freight markets, energy and import prices, and U.S. inflation. Section 4 develops a multi-country general equilibrium model in which shipping disruptions operate through increases in trade costs. Section 5 presents the quantitative results, and Section 6 uses the model to study the Red Sea Crisis and the closure of the Strait of Hormuz under alternative monetary policy rules. Section 7 concludes.

2 Background, Data, and Measurement of Chokepoint Disruptions

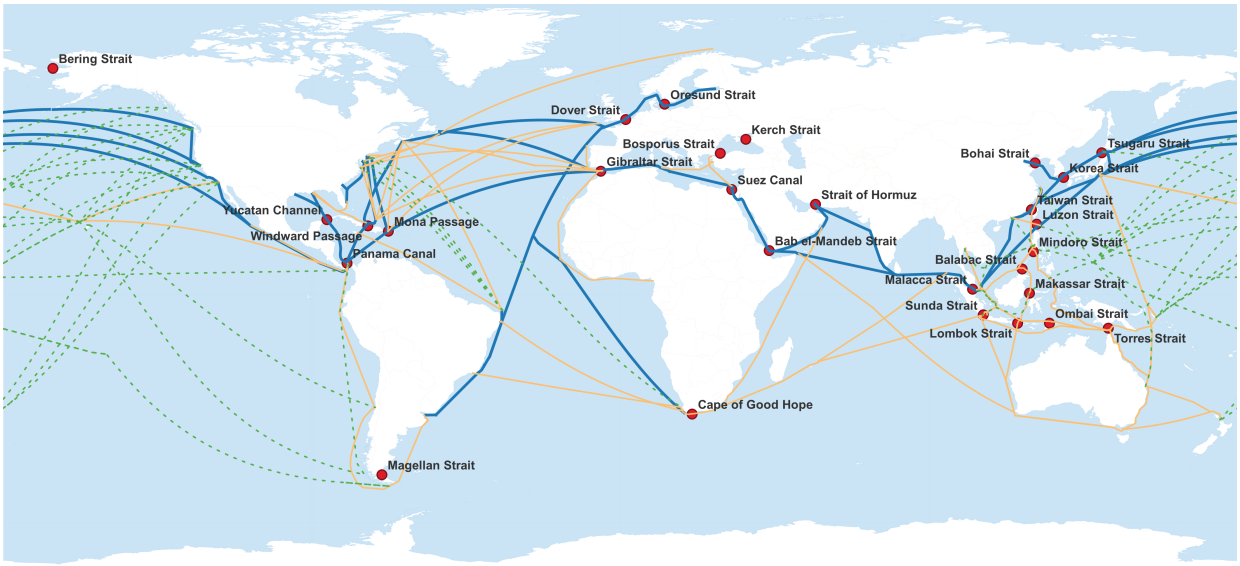
This section provides the background, data, and measurement framework for our empirical analysis. We first describe the role of maritime chokepoints in global shipping and the sources of disruptions to vessel traffic. We then introduce the data used in the analysis. Using recent disruption episodes, we document that chokepoint disruptions affect multiple freight categories and induce substantial rerouting across the maritime network. These patterns motivate our construction of a global maritime chokepoint disruption index that summarizes changes in shipping activity across chokepoints and freight categories.

2.1 Maritime Chokepoints and Shipping Disruptions

Maritime shipping is the backbone of global goods trade: more than 80 percent of the volume of international merchandise trade is transported by sea (UNCTAD, 2025). A key feature of this system is its reliance on maritime chokepoints—geographically narrow or constrained passages through which large volumes of commercial vessel traffic flow (Figure 1). Prominent examples include the Suez Canal, the Strait of Hormuz, and the Panama Canal. Because vessel flows are highly concentrated at these locations and alternative routes are often limited, disruptions at chokepoints can have consequences for global trade that extend well beyond the countries or ports located nearby.

Maritime chokepoint disruptions can take several forms. In some cases, vessel traffic is restricted by geopolitical conflict or sanction enforcement. Even when vessels are not fully prevented from transiting, heightened risk or uncertainty can reduce traffic. A recent example is the Red Sea disruption beginning in late 2023 following attacks by Yemen's Houthi movement on commercial vessels in the Red Sea and Gulf of Aden (the *Red Sea Crisis*). As security risks increased, many carriers avoided the Suez-Canal-Bab el-Mandeb-Strait corridor and rerouted around the Cape of Good Hope. Another more recent episode is the Strait of Hormuz disruption starting in March 2026, when military escalation in the Middle East sharply reduced ship transits through the narrow passage connecting the Persian Gulf to the Gulf of Oman.

Figure 1: Maritime Chokepoints and Global Shipping Routes



Notes: Red circles mark major maritime chokepoints worldwide. Lines show shipping routes: blue for major routes, orange for medium routes, and green dashed for minor routes. The map was constructed by the authors using chokepoint locations from the IMF PortWatch Ports and Chokepoints Dataset and shipping routes and route categories from Benden (2022).

In other cases, disruptions arise from operational constraints caused by natural disasters, climate change, or accidents. For instance, in 2023 and 2024, persistent drought conditions lowered water levels in the Panama Canal, severely restricting vessel traffic and daily crossings. Likewise, accidents often temporarily reduce a canal's capacity. In March 2021, for example, the container ship *Ever Given* ran aground and blocked traffic through the Suez Canal for six days.

These episodes show that disruptions at maritime chokepoints can affect U.S. inflation through channels distinct from those associated with trade policy shocks or energy price shocks. As we show in the next section, by reducing effective shipping capacity, these shocks raise freight rates, increase import prices, and drive up intermediate input costs. This important distinction motivates the approach in our paper. We measure chokepoint disruptions using data on vessel movements, isolate maritime shipping shocks with a structural VAR model, and study their transmission mechanisms and monetary policy implications through the lens of a quantitative model.

2.2 Data

Our empirical analysis combines three sets of data. The first is a novel daily dataset on physical vessel movements through global maritime chokepoints. The second consists of freight rate indexes that measure price responses in different shipping markets (e.g., container, dry-bulk, and tanker markets). The third includes U.S. and global macroeconomic variables used to study

the transmission of shipping disruptions to inflation and economic activity.

Chokepoint Transit Calls and Trade Volume. Our main data source is the IMF PortWatch Daily Chokepoint Transit Calls and Trade Volume Estimates. PortWatch is an open platform that uses satellite-based vessel tracking data from the Automatic Identification System (AIS) to monitor maritime trade flows in near real time.[5] The dataset contains the number of vessel transits and estimated trade volumes for 28 major chokepoints around the world (Figure 1), with information available at the chokepoint level by vessel category.[6]

The key advantage of the PortWatch data is that they capture physical shipping activity close to the source of the disruption. By contrast, shipping rates are useful indicators of market prices, but they are equilibrium outcomes that reflect both supply and demand conditions (e.g., Känzig and Raghavan 2026). Similarly, broader supply chain indexes summarize many frictions in survey data but do not isolate the maritime component (e.g., Benigno et al. 2022). This distinction is important for identification. In our empirical analysis, we employ PortWatch data to construct the maritime disruption measure, while using shipping rates and aggregate prices as outcome variables. To our knowledge, this paper is the first to use the chokepoint-level transit trade volume data to construct a global network-wide disruption measure and study its macroeconomic effects.

Shipping Rates. The second set of data includes shipping freight rates obtained from Bloomberg Finance L.P. For container shipping, we use the Drewry World Container Index and the Shanghai Containerized Freight Index. The former reports weekly spot container freight rates for major East-West trade routes, with rates reported in U.S. dollars per 40-foot container. The latter measures spot freight rates in the Shanghai export container market. These two indexes provide complementary measures of container-market pricing, one capturing major global routes, while the other focusing on export rates from Shanghai—one of the most important container-shipping origins.

For non-container shipping, we use Baltic Exchange freight indexes, which provide benchmarks

[5] AIS is mandated by the International Maritime Organization (IMO) for international ships exceeding 300 gross tons. Bai et al. (2026b) document that more than 99% of international container shipments are carried by vessels above 500 gross tons, and even very small vessels (below 300 gross tons) usually carry AIS. Our data capture the large commercial fleet most relevant for international trade, but they may be incomplete for vessels that deactivate or manipulate AIS signals.

[6] AIS does not directly report cargo volumes or trade values. PortWatch first estimates vessel-level shipment volumes (in metric tons) using AIS-reported information together with vessel characteristics, following methodology in Arslanalp et al. (2025) and Arslanalp et al. (2021), and then aggregates the estimated volumes carried by vessels observed transiting each chokepoint to obtain chokepoint-level transit-volume estimates. These estimates should be interpreted as proxies for maritime trade and may differ from official customs statistics. Our disruption measure in Section 2.3, however, is less sensitive to potential discrepancies in these trade-volume estimates, because it is constructed from deviations from a pre-period benchmark within the same chokepoint and vessel category. Any time-invariant or slowly moving measurement discrepancies are therefore differenced out.

for dry-bulk and tanker markets. The Baltic Dry Index summarizes dry-bulk freight market conditions and is constructed from Capesize, Panamax, and Supramax time charter averages. We also use tanker-related Baltic indexes to capture shipping costs for refined petroleum products. Together, these container and non-container indexes allow us to examine whether a typical chokepoint disruption transmits broadly across shipping markets.

U.S. Macroeconomic Variables. The third set of data consists of U.S. macroeconomic variables. Our main inflation outcomes are U.S. consumer and producer price indexes, as well as import prices, from the Bureau of Economic Analysis and the Bureau of Labor Statistics. We also use energy price data from the Energy Information Administration, such as crude oil prices and retail gasoline prices, to distinguish maritime shipping shocks from conventional energy price shocks. To assess the responses of monetary policy, we obtain U.S. Treasury yield data from FRED. Our sample starts in January 2019, when PortWatch chokepoint data are available, and extends through June 2026, the latest month available in our data extract.

2.3 Measuring Maritime Chokepoint Disruptions

This subsection first presents stylized facts on shipping flows around major chokepoint disruptions, then proposes a monthly measure of maritime disruptions that aggregates information across chokepoints, and finally compares it with alternative measures of supply chain pressure.

2.3.1 Narrative Evidence

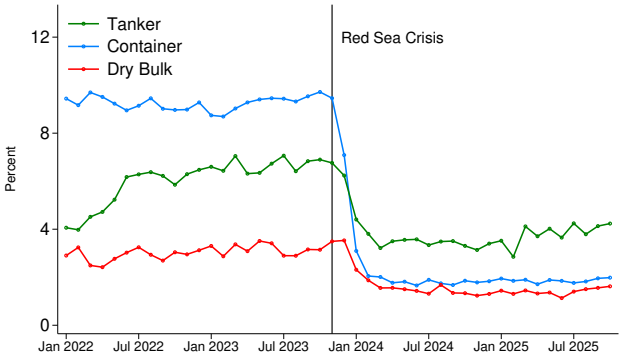
Before constructing a global measure of maritime chokepoint disruptions, we first use recent episodes to illustrate how disruptions appear in high-frequency chokepoint-level data. We focus on two major episodes—the Red Sea Crisis beginning in November 2023 and the U.S.–Iran War beginning in March 2026—and present additional episodes in Appendix A.1. For each episode and chokepoint, we measure traffic as the transit trade volume as a share of global shipment volume, separately for each vessel category. We use monthly data for most episodes, while relying on daily data for the very recent U.S.–Iran War and the short-lived *Ever Given* grounding incident. This exercise documents two features that guide our measurement strategy.

Fact 1. Major chokepoint disruptions affect shipping flows across all freight categories.

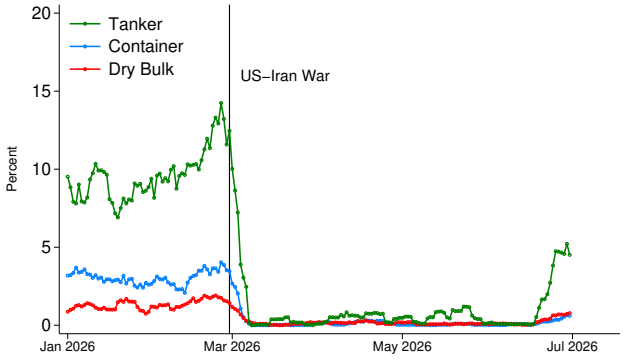
Figure 2 plots transit trade volumes through the Suez Canal around the Red Sea Crisis (panel a) and through the Strait of Hormuz around the 2026 U.S.–Iran War (panel b). In both cases, transit volumes fell sharply at the affected chokepoint, and the declines were not limited to the vessel category most directly associated with the event. At the Suez Canal, the share of global shipping volume transiting through the canal declined from the pre-crisis period to early 2024 by approximately 7 percentage points (pp) for container trade, 3 pp for tanker trade, and 2 pp for

Figure 2: Transit Trade Volume Responses to Chokepoint Disruptions

(a) Suez Canal



(b) Strait of Hormuz



Source: IMF PortWatch Daily Chokepoint Transit Calls and Trade Volume Dataset. Notes: The figure shows transit trade volume through each chokepoint as a share of global shipping volume, by freight category. Trade volume data underlying panel (a) are monthly aggregates constructed from daily observations, while data underlying panel (b) are seven-day moving averages.

dry-bulk trade.[7] The disruption had a persistent effect on shipping activity, as flows through this route had not recovered by early 2026.

Similarly, following Iran's blockage of the Strait of Hormuz in March 2026, shipments across all freight categories came to a near halt. Only a small fraction of traffic resumed after the U.S. and Iran signed a "memorandum of understanding" in late June aimed at de-escalating tensions. Although the Hormuz disruption is often discussed primarily in the context of energy shipments, just as the Suez disruption is commonly associated with container shipping, the data show broad-based declines in container, tanker, and dry-bulk traffic in both episodes. This pattern motivates constructing a disruption measure that aggregates information across freight categories.

Fact 2. Disruptions at one chokepoint often spill over to other parts of the maritime network.

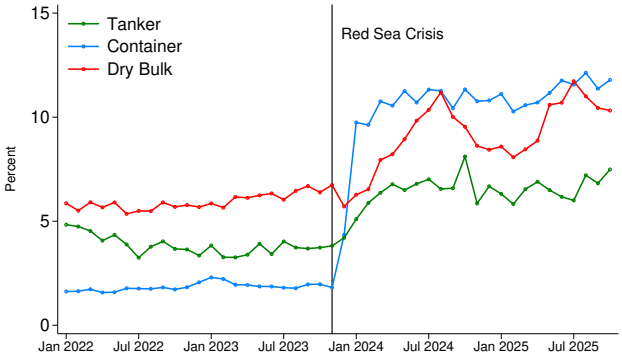
Figure 3 shows that, following the Red Sea Crisis, traffic increased around the Cape of Good Hope as carriers avoided the Suez–Bab el-Mandeb corridor and rerouted vessels around southern Africa (panel a). Panel (b) documents a similar spillover during the 2026 Middle East escalation: tanker traffic increased through the Yucatan Channel that connects the Caribbean Sea with the Gulf of Mexico, as importers substituted toward crude oil and refined petroleum products supplied by the U.S. Gulf Coast in response to reduced shipments from the Middle East.

These spillovers imply that the effects of a chokepoint disruption are not fully captured by

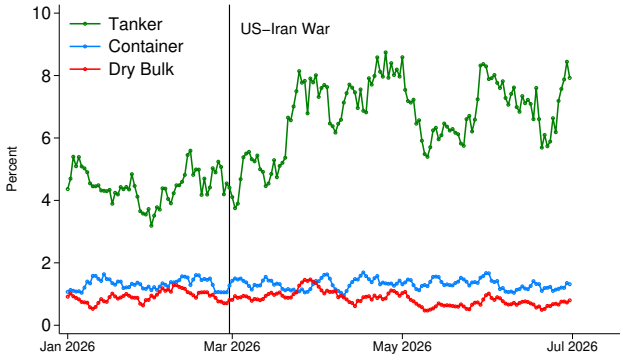
[7] Our measure of container transit trade volume includes shipments carried by container ships, roll-on/roll-off (Ro-Ro) ships, and general cargo ships. We group these vessel types because they predominantly carry manufactured and other non-bulk goods, in contrast to tanker and dry-bulk vessels. The latter two vessel types account for only about 2% of the combined transit trade volume across these categories.

Figure 3: Spillovers of Chokepoint Disruptions to Other Maritime Passages

(a) Cape of Good Hope



(b) Yucatan Channel



Source: IMF PortWatch Daily Chokepoint Transit Calls and Trade Volume Dataset. Notes: The figure shows transit trade volume through each chokepoint as a share of global shipping volume, by freight category. Trade volume data underlying panel (a) are monthly aggregates constructed from daily observations, while data underlying panel (b) are seven-day moving averages.

the decline in traffic at the affected passage. A localized shock can alter vessel flows at distant chokepoints through rerouting and supply chain reallocation. These adjustments can raise shipping costs not only by increasing voyage distances, but also by tightening capacity and raising freight rates along alternative routes as demand for those routes increases.

In Appendix A.1, we present additional evidence from several smaller-scale or short-lived chokepoint disruptions: (i) the grounding of the *Ever Given* in 2021, which temporarily blocked the Suez Canal, (ii) the 2022 Russia–Ukraine War, which reduced transits through the Bosporus Strait, and (iii) the 2023 Panama Canal disruption caused by severe drought. Similar to patterns shown in Figure 2, shipping volumes declined across multiple freight categories in each of these episodes. However, because these episodes were relatively short-lived or limited in scale, the resulting rerouting is not clearly visible in the data.

Together, these patterns motivate our construction of a global maritime chokepoint disruption index that captures both declines in the use of directly affected routes and the reallocation of traffic from these routes to alternative routes. A measure based on a single vessel category would also miss the broad-based nature of major disruptions. We therefore construct our baseline index that accounts for both dimensions and measures maritime disruptions consistently over time, as described next.

2.3.2 Constructing the Maritime Chokepoint Disruption (MCD) Index

To measure maritime chokepoint disruptions, we construct a monthly index that aggregates information across chokepoints. The index is designed to capture both direct disruptions at affected

chokepoints and spillovers arising from rerouting and the reallocation of shipping activity across the maritime network. First, for each freight category $f \in \{C, D, T\}$ and month t, define chokepoint c's share of total transit trade volume across global major chokepoints as

$$S_t^{c,f} \equiv \frac{V_t^{c,f}}{\sum_k V_t^{k,f}}, \quad \sum_c S_t^{c,f} = 1,$$

where $V_t^{c,f}$ denotes the transit trade volume of freight category f passing through chokepoint c in month t; C, D and T denote container, dry-bulk and tanker trade, respectively. We then construct the raw MCD measure for month t by aggregating the absolute deviations of $S_t^{c,f}$ from the corresponding benchmark shares $S_0^{c,f}$ across chokepoints and freight categories:

$$MCD_t^{raw} = \sum_{f \in \{C,D,T\}} \bar{w}_{t-12}^{f} \frac{1}{2} \sum_c \left| S_t^{c,f} - S_0^{c,f} \right|. \tag{1}$$

Our baseline specification sets $S_0^{c,f}$ equal to the average monthly share in 2019, and our results are robust to alternative benchmark periods.[8]

$\bar{w}_{t-12}^{f}$ denotes the weight assigned to freight category f, defined as its average share of U.S. seaborne trade value over the 12 months preceding month t, using monthly international trade data from the U.S. Census Bureau. We use U.S. trade-value shares as a high-frequency proxy for the relative economic importance of the three freight categories in global seaborne trade.[9] Using a trailing 12-month average smooths short-run fluctuations in trade composition and ensures that the weights are predetermined relative to shipping conditions in month t.

The MCD measure is straightforward to interpret. For a given freight category, the term $\frac{1}{2} \sum_c \left| S_t^{c,f} - S_0^{c,f} \right|$ equals zero if the transit volume share at every chokepoint is unchanged from its 2019 level, and is positive whenever the share at one or more chokepoints deviates from that benchmark. We note that the use of summed absolute deviations has close precedents in the

[8] Because transit shipping volumes exhibit clear seasonality, we seasonally adjust the volume variables using panel regressions that include calendar-month fixed effects, chokepoint fixed effects, and chokepoint-specific linear time trends. This specification removes common seasonal patterns while allowing long-run trends to vary across chokepoints.

[9] Ideally, the weights would be based on monthly global seaborne trade values by freight category, but comparable global data are considerably more limited. The U.S. Census Bureau provides consistently measured monthly vessel trade values and directly identifies containerized trade at detailed product levels. We identify tanker and dry-bulk trade using Harmonized System (HS) codes, following Cerdeiro et al. (2020). Over our sample period, container (including Ro-Ro and general-cargo), tanker, and dry-bulk shipments account for approximately 75%, 19%, and 6%, respectively, of U.S. vessel-borne trade value. Our results are robust to using fixed weights equal to these sample-average shares instead of trailing 12-month averages, as well as to alternative weights of 60%, 30%, and 10% for container, tanker, and dry-bulk shipping, respectively.

labor economics literature on sectoral reallocation.[10] As is standard in this literature, the factor of one-half avoids double-counting reallocation.

In equation (1), we use transit trade volume *shares* rather than *levels*, because traffic through a chokepoint reflects not only route-specific conditions, but also changes in global shipping driven by aggregate expansions or contractions in trade. Using shares within each freight category helps remove the effects of endogenous global business cycles, provided that these cycles do not alter the distribution of traffic flows across chokepoints.[11] The absolute-value operator serves a separate purpose, allowing the index to capture both declines in traffic through directly affected chokepoints and increases along alternative routes or through chokepoints serving substitute suppliers.

Finally, we first-difference the raw measure in equation (1) to focus on changes in maritime disruption intensity rather than persistent differences from the benchmark shipping pattern, and standardize the resulting series as shown in equation (2). In Section 3 we identify maritime chokepoint disruption shocks from innovations to this measure:

$$MCD_t = \frac{\Delta MCD_t^{raw} - \overline{\Delta MCD_t^{raw}}}{sd(\Delta MCD_t^{raw})}. \tag{2}$$

Panel (a) of Figure 4 plots the raw and standardized MCD indexes beginning in 2019. The indexes exhibit substantial variation over time, reflecting idiosyncratic disruptions at the chokepoint level. Two episodes stand out. The first is the Red Sea Crisis, during which the indexes show persistent and intensifying disruptions from December 2023 through mid-2024 before stabilizing. The second is the recent closure of the Strait of Hormuz. In panel (b), we plot a disruption index using container transit trade volume data only (blue), given its dominant role in the value of global seaborne trade. The container and overall indexes are highly correlated, with a correlation coefficient of 0.86 over our sample, suggesting that container shipping disruptions play an important role in driving overall maritime chokepoint disruptions.

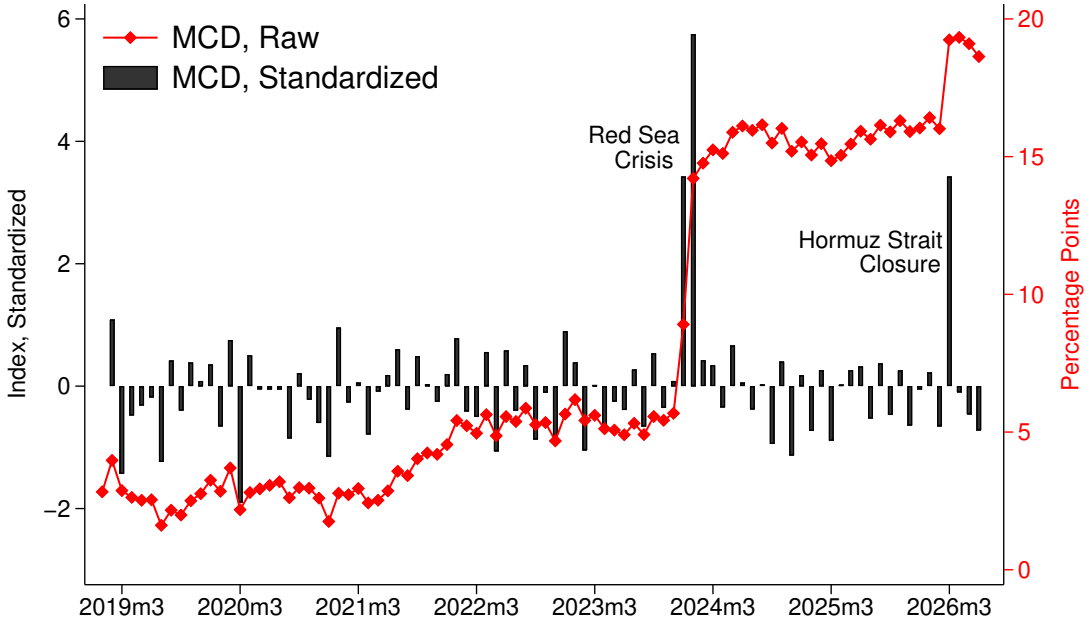
The substantial variation in our maritime chokepoint disruption measures motivates our use of a structural VAR model to quantify the macroeconomic implications of chokepoint disruptions for U.S. inflation. Our baseline estimates use the overall MCD index, as the evidence in Section 2.3.1 shows that chokepoint disruptions affect shipping across all freight categories. Nevertheless, we

[10] For example, Kambourov (2009) and Chodorow-Reich and Wieland (2020) measure sectoral labor reallocation using one-half of the sum of absolute changes in sectoral employment shares. Forsythe et al. (2022) similarly measure employment reallocation following the COVID-19 shock using one-half of the sum of absolute deviations in employment shares from a benchmark period. Our index applies the same absolute-deviation logic to maritime traffic shares across chokepoints and freight categories.

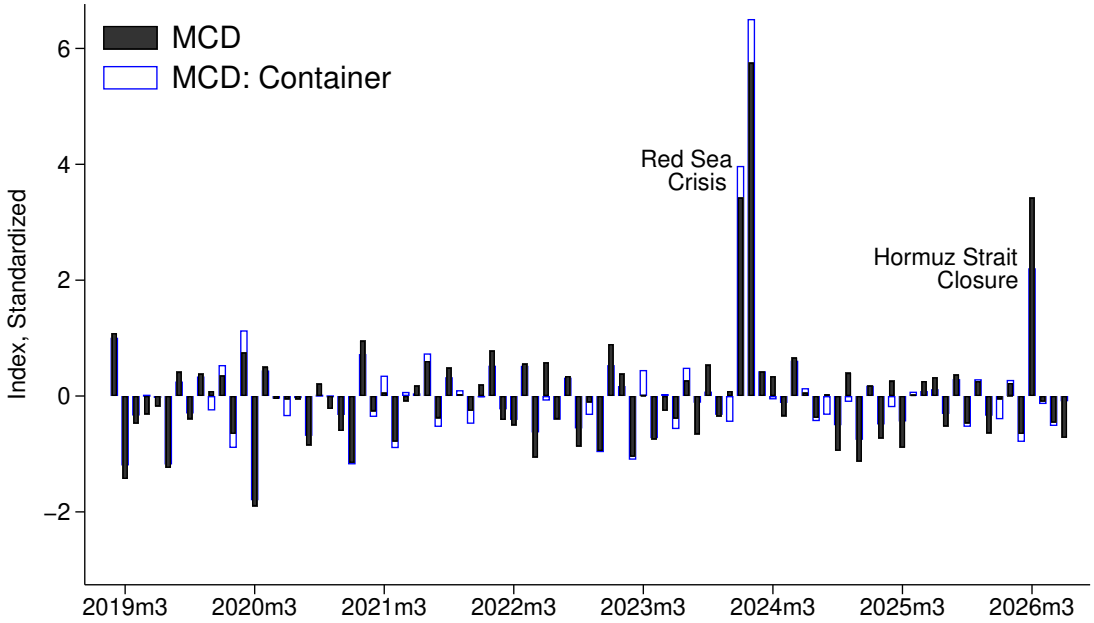
[11] Using shares reduces, but does not completely eliminate, potential demand-related variation. A route-specific demand shift or a change in the geographic composition of global trade could still alter chokepoint shares even without a physical disruption. Our SVAR identification and robustness analysis address this remaining concern.

Figure 4: Measures of Maritime Chokepoint Disruptions (MCD)

(a) Overall Index



(b) Overall vs. Container Indexes



Notes: The raw and standardized maritime chokepoint disruption (MCD) indexes are constructed according to equations (1) and (2), respectively. The MCD-Container index is constructed analogously to the standardized MCD index, using only container transit trade volume data.

show that our results are robust to using the container-only index.

2.3.3 Comparison with Alternative Measures of Supply Chain Disruptions

The MCD index is designed to capture one specific type of global supply chain disruption: physical disruptions to maritime shipping that propagate through the network of chokepoints. Other indicators may reflect such disruptions, but they also reflect other sources of supply chain stress, including port congestion, input and labor shortages, and shifts in demand. Figure 5 compares the MCD index with four such measures: (a) the average rerouting distance of U.S.-bound container vessels from Asia Pacific and from the Middle East to the U.S. East Coast, defined as the extra nautical miles sailed relative to the shortest route (Bai et al., 2026a); (b) monthly changes in the Shanghai Containerized Freight Index; (c) the Global Supply Chain Pressure Index (GSCPI) of Benigno et al. (2022); and (d) the average port congestion rate (ACR) of Bai et al. (2026b).

The MCD index is positively correlated with the first two measures (about 0.28 with rerouting distances and 0.40 with freight rate changes).[12] Rerouting distances were flat until late 2023 and rose sharply when carriers diverted vessels around the Cape of Good Hope at the onset of the Red Sea Crisis, coinciding with the largest spike in the MCD index. The largest increases in container freight rates likewise coincide with the MCD spikes at the onset of the Red Sea Crisis and the closure of the Strait of Hormuz.

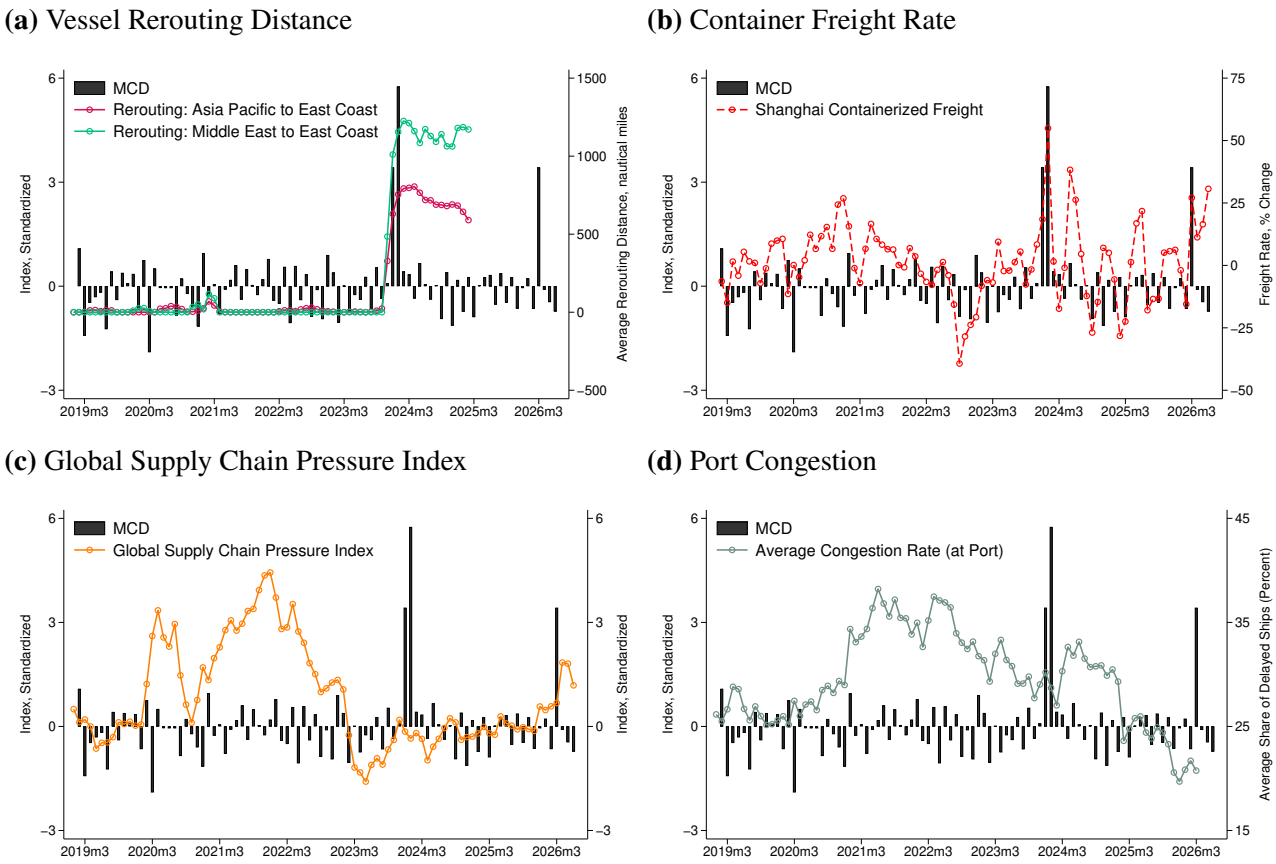
By contrast, the MCD index is essentially uncorrelated with the GSCPI (-0.04) and with port congestion (-0.05). The GSCPI combines transportation costs and survey-based indicators of delivery times, backlogs, and inventories (adjusted for demand proxies), while ACR measures the share of container-ship visits subject to delays at major ports. Both indicators show pronounced strains during the pandemic, in contrast to the concentration of large MCD spikes around major chokepoint disruptions. This divergence is consistent with the different dimensions of supply chain disruption being measured. Our MCD index therefore complements existing indicators by distinguishing disruptions to maritime routes from congestion at ports and pressures elsewhere along the supply chain.

3 Empirical Evidence

Having constructed a measure of maritime chokepoint disruptions, we use a structural VAR model to estimate the effects of shipping disruption shocks on U.S. inflation. The SVAR serves two purposes. First, because shipping rates, commodity prices, inflation, and monetary policy co-move,

[12] Rerouting distances are plotted in levels (as in Figure 3.3 of Bai et al. 2026a), whereas MCD is the standardized first difference of the raw disruption index. The correlations with MCD increase to approximately 0.45 when the rerouting-distance series are also first-differenced.

Figure 5: MCD and Alternative Supply Chain Disruption Measures



Source: IMF PortWatch Daily Chokepoint Transit Calls and Trade Volume Dataset; Shanghai Containerized Freight Rate (Bloomberg Finance L.P.); New York Fed Global Supply Chain Pressure Index; Average Congestion Rate from Bai et al. (2026b); Average Rerouting Distances from Bai et al. (2026a).

the model allows us to isolate exogenous variation in maritime chokepoint disruptions and trace its dynamic effects on inflation. Second, by examining the responses of a broader set of macroeconomic variables, we provide evidence on the transmission channels through which chokepoint disruptions affect the economy. These empirical patterns, in turn, motivate the theoretical model developed in Section 4. We first describe the empirical framework, with particular emphasis on identification and estimation, and then present the baseline inflation results, the responses of broader macroeconomic outcomes, and a series of robustness checks.

3.1 Structural VAR Model: Identification and Estimation

Our empirical framework follows Rubio-Ramírez et al. (2010) and Kilian and Lütkepohl (2017), and is also related to the recent SVAR literature on identifying the causal effects of energy price shocks on U.S. inflation (e.g., Kilian and Zhou 2022a,b, 2025). The structural VAR model can be

written as

$$\mathbf{B_0} y_t = \mathbf{B_1} y_{t-1} + \cdots + \mathbf{B_p} y_{t-p} + \varepsilon_t,$$

where y_t is an $n \times 1$ vector of endogenous variables, ε_t is an $n \times 1$ vector of mutually uncorrelated i.i.d. structural shocks, and $\mathbf{B_i}$, $i = 0, \ldots, p$, denote $n \times n$ coefficient matrices. The intercept is suppressed for expository purposes. The corresponding reduced-form VAR model representation is

$$y_t = \mathbf{A_1} y_{t-1} + \cdots + \mathbf{A_p} y_{t-p} + u_t,$$

where $\mathbf{A_i} = \mathbf{B}_0^{-1}\mathbf{B_i}$, $i = 1, \ldots, p$, and $u_t = \mathbf{B}_0^{-1}\varepsilon_t$. We set the lag order $p = 6$ in the baseline model.

The baseline SVAR contains five monthly variables: the standardized maritime chokepoint disruption index, MCD, constructed in Section 2.3, the WTI crude oil price, the PCE chain-type price index, the core PCE price index (PCE excluding food and energy), and the one-year U.S. Treasury yield as a measure of the short-term interest rate. As discussed below, we also examine the responses of a broader set of U.S. and global macroeconomic variables, including the U.S. producer price index, U.S. import prices, container and non-container freight rates, and global transit shipping volumes. All variables enter the model in log levels except the MCD index and the short-term interest rate.

Identification. Our primary interest is in the causal effects of a maritime chokepoint disruption shock. As such, we only partially identify the model, focusing on this shock rather than identifying the full set of structural shocks. The estimated responses to the maritime chokepoint disruption shock are invariant to the identification of the remaining structural shocks (Christiano et al. 1999). The identification is based on the assumption that innovations to the maritime chokepoint disruption index are predetermined with respect to other variables in the model within a month. This assumption is supported by the narrative evidence in Section 2.3.1, which shows that major chokepoint disruptions are triggered by unexpected geopolitical conflicts, natural disasters or accidents, rather than by endogenous responses to U.S. economic conditions or oil price fluctuations. Under this identifying assumption,

$$\begin{pmatrix} u_t^{MCD} \\ u_t^{Oil} \\ u_t^{PCE} \\ u_t^{PCE,core} \\ u_t^{R} \end{pmatrix} = \begin{bmatrix} * & 0 & 0 & 0 & 0 \\ * & * & * & * & * \\ * & * & * & * & * \\ * & * & * & * & * \\ * & * & * & * & * \end{bmatrix} \begin{pmatrix} \varepsilon_t^{\text{Shipping Disruption}} \\ \varepsilon_t^2 \\ \varepsilon_t^3 \\ \varepsilon_t^4 \\ \varepsilon_t^5 \end{pmatrix},$$

where stars denote elements of $\mathbf{B_0}^{-1}$ that remain unrestricted.

Estimation. We estimate the model using the Bayesian approach described in Arias et al. (2018)

and postulate a diffuse Gaussian-inverse Wishart prior for the reduced-form parameters (see also Kilian and Zhou 2022a). The prior of the VAR slope parameter vector is $\beta \sim N(0, \Sigma \otimes \Omega_0)$, where Ω_0 is a diagonal matrix with j^{th} diagonal element $(1/\sigma_j^2)(0.2/l)^2$, σ_j^2 is approximated as the residual variance of an AR(1) regression for variable j, l indicates the lag, and $\Sigma \sim IW(S_0, \alpha_0)$ with $\alpha_0 = 7$ and $S_0 = (\alpha_0 - 5 - 1)\,\text{diag}\left(\sigma_1^2, \sigma_2^2, \sigma_3^2, \sigma_4^2, \sigma_5^2\right)$. All results are based on 10,000 posterior draws.

Finally, to examine the responses of a broader set of macroeconomic outcomes, we replace the core PCE price index in the baseline SVAR with one outcome variable at a time, leaving the remaining variables unchanged. This rotating-variable approach is widely used in the structural VAR literature (e.g., Christiano et al. 1996; Ramey 2011; Gertler and Karadi 2015).

3.2 Impulse Responses

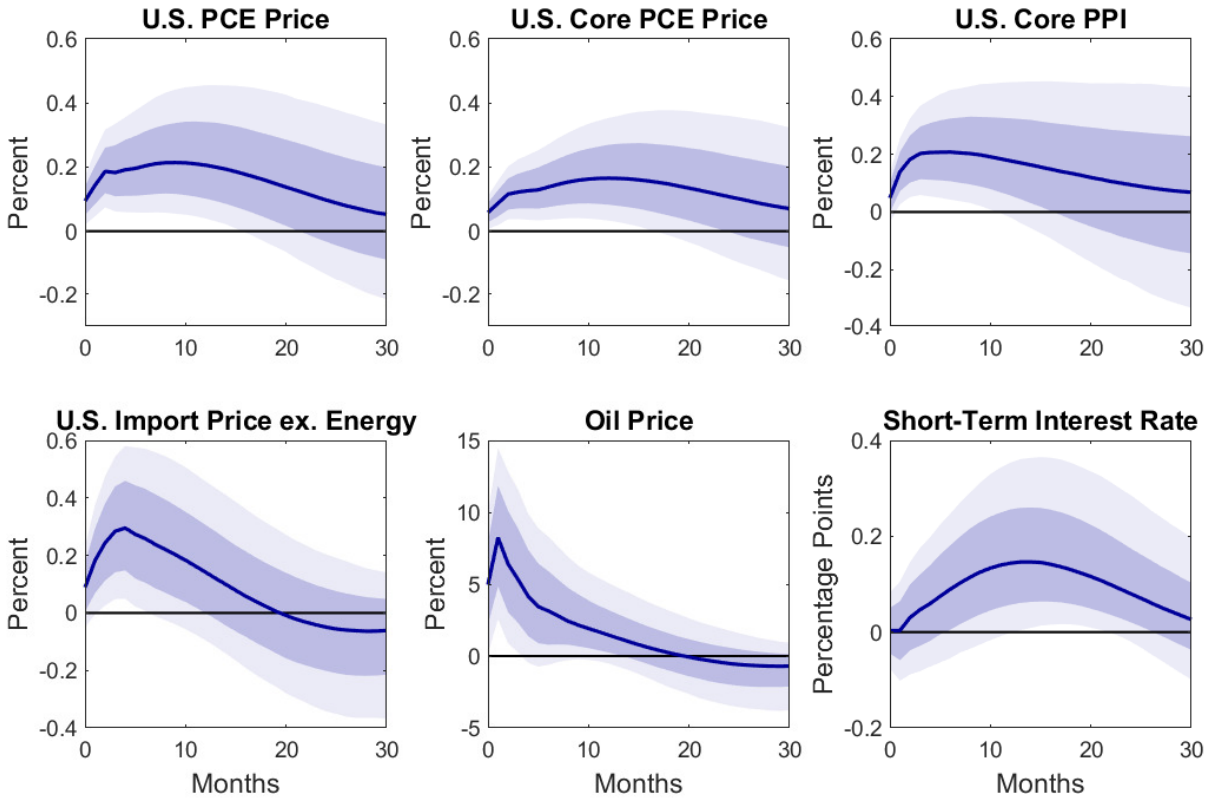
Baseline Results. Figure 6 shows the responses of key endogenous variables to an adverse maritime chokepoint disruption shock. The solid lines indicate pointwise posterior median impulse responses, while the shaded areas indicate the 68% and 90% posterior credible sets. We normalize the shock to raise the MCD index by two standard deviations on impact. This normalization is intended to capture a large disruption of the magnitude typically associated with major chokepoint events in the data (see Figure 4).

The upper panels of Figure 6 show that an adverse maritime chokepoint disruption raises U.S. consumer prices persistently. The response remains credibly positive for about 20 months and peaks at approximately 0.21 percent after ten months. Much of this increase is accounted for by core prices, suggesting that the effects of shipping disruptions extend beyond their direct impact on energy and other volatile components of consumer prices. Producer prices also rise substantially: the core PPI response peaks at about 0.21 percent after seven months and remains credibly positive over much of the first year following the shock.

The lower panels provide evidence on several channels underlying these price responses. Import prices excluding energy rise for roughly one year following the shock, consistent with pass-through of higher international transportation costs to the prices of imported goods, a channel we examine in more detail below. The shock also raises energy prices, including the WTI oil price and U.S. retail gasoline prices. Finally, the short-term interest rate increases with a lag of several months, consistent with a monetary policy response to the resulting inflationary pressures.

Figure 7 presents the responses of global shipping rates and volumes to an adverse maritime chokepoint disruption shock. The upper panels show sizable and broad-based increases in container freight rates. The middle panels report the responses of non-container freight rates. Clean tanker freight rates—which capture the cost of transporting refined petroleum products such as gasoline,

Figure 6: Impulse Responses to Maritime Chokepoint Disruption Shocks

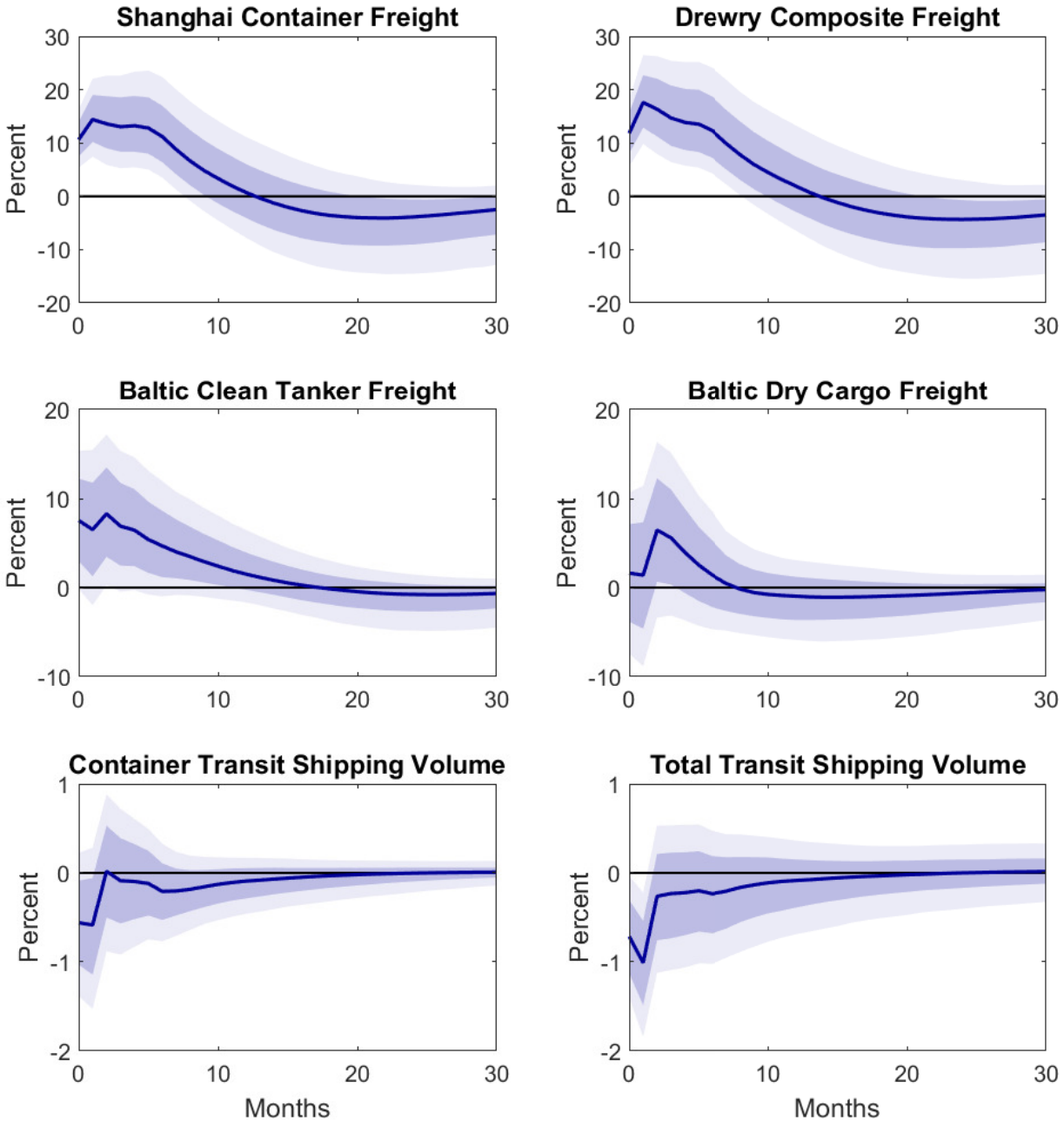


Notes: The solid lines indicate pointwise posterior median impulse response functions, and the shaded areas indicate the 68% and 90% posterior credible sets. The IRFs are responses to an adverse two-standard-deviation shock to the maritime chokepoint disruption (MCD) index.

diesel, and jet fuel—increase sharply on impact and remain credibly elevated, whereas the response of dry-bulk freight rates is comparatively modest. On the quantity side, the lower panels show declines in transit shipping volumes for both containerized and non-containerized goods.

Taken together, these responses are consistent with maritime chokepoint disruptions operating as an adverse supply shock: they reduce global shipping volumes, while raising shipping rates, import prices, and energy prices, and these cost pressures ultimately pass through to U.S. producer and consumer prices. These sign patterns are not imposed by our identification, which relies only on the timing of chokepoint disruptions; they emerge from the data. Our approach thus complements studies that identify supply chain shocks from sign restrictions or freight rate movements (e.g., Bai et al. 2026b; Känzig and Raghavan 2026), which build in the assumption that adverse shipping shocks raise rates and reduce volumes. Because we do not impose this assumption, the negative co-movement of shipping rates and quantities in our estimates confirms the supply nature of the shock ex post.

Figure 7: Shipping Market Responses to Maritime Chokepoint Disruption Shocks



Notes: The solid lines indicate pointwise posterior median impulse response functions, and the shaded areas indicate the 68% and 90% posterior credible sets. The IRFs are responses to an adverse two-standard-deviation shock to the maritime chokepoint disruption (MCD) index.

Robustness. Our baseline results are robust to alternative measures of maritime chokepoint

disruptions and energy prices, different sample periods, and alternative model specifications. Figure 8 reports three key robustness checks, with additional results relegated to Appendix A.2. First, we replace the baseline MCD index with the MCD-Container index. This specification addresses potential changes in the composition of freight types most affected by chokepoint disruptions. Second, we increase the lag order from 6 to 12 months to allow for richer delayed dynamics among the model variables. Third, we exclude the recent closure of the Strait of Hormuz by ending the sample in February 2026. Across all three exercises, the estimated responses are little changed relative to the baseline.

Appendix A.2 reports additional robustness checks. Specifically, we consider alternative measures of energy prices (panel a) and short-term interest rates (panel b), as well as a specification in which the relevant variables enter in growth rates (panel d). We also show that our results are robust to excluding the major variation associated with both the Red Sea Crisis and the Strait of Hormuz closure (panel c). Specifically, we end the sample in February 2026 to exclude the Strait of Hormuz episode. To remove the initial spike associated with the onset of the Red Sea Crisis, we replace the MCD index in December 2023 and January 2024 (the first pronounced spikes in Figure 4) with values obtained by linear interpolation between November 2023 and February 2024, thereby smoothing out this episode. Our baseline results remain robust.

4 Model

Motivated by the empirical evidence in Section 3, we adapt the model of Cuba-Borda et al. (2025) to study the macroeconomic effects of maritime chokepoint disruptions. The world consists of N countries indexed by $i, h \in \mathcal{I} = \{1, \ldots, N\}$, each with population ξ_i, with world population normalized to one in every period. Country 1 is the United States, and time is indexed by $t = 1, 2, \ldots$.

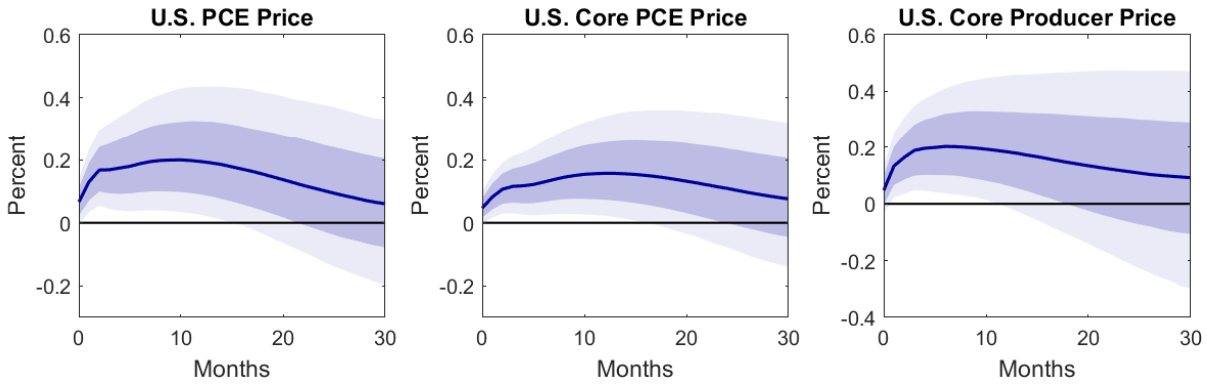
Each country produces a single tradable good, differentiated by country of origin, that can be bought by households and firms in every country: households buy it for final consumption and firms buy it as an intermediate input. Countries also trade a single financial asset, a risk-free bond denominated in (real) dollars, country 1's currency, so international financial markets are incomplete. Apart from this role of country 1's currency, all countries share the same structure, and we describe a generic country i.

4.1 Households

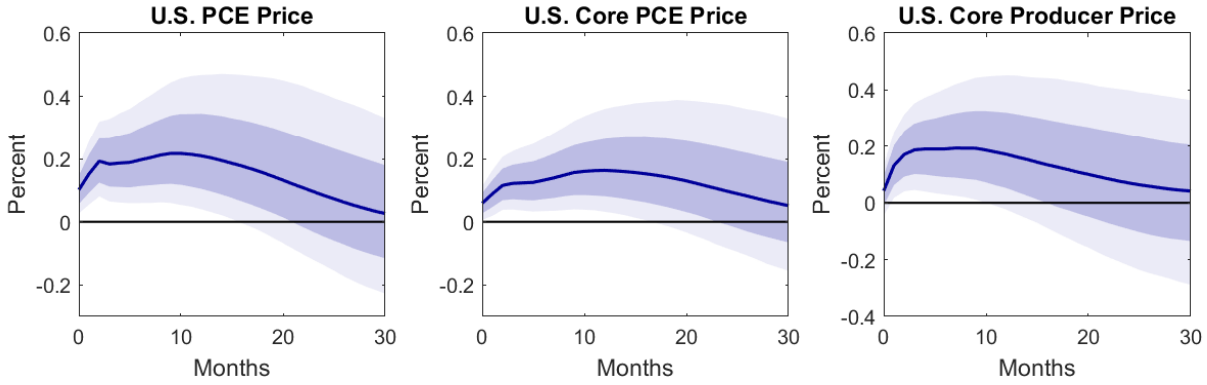
Each country has a continuum of households indexed by ℓ. Households supply differentiated labor services to firms under monopolistic competition, as in Erceg et al. (2000). Household ℓ in

Figure 8: Robustness of U.S. Consumer and Producer Price Responses

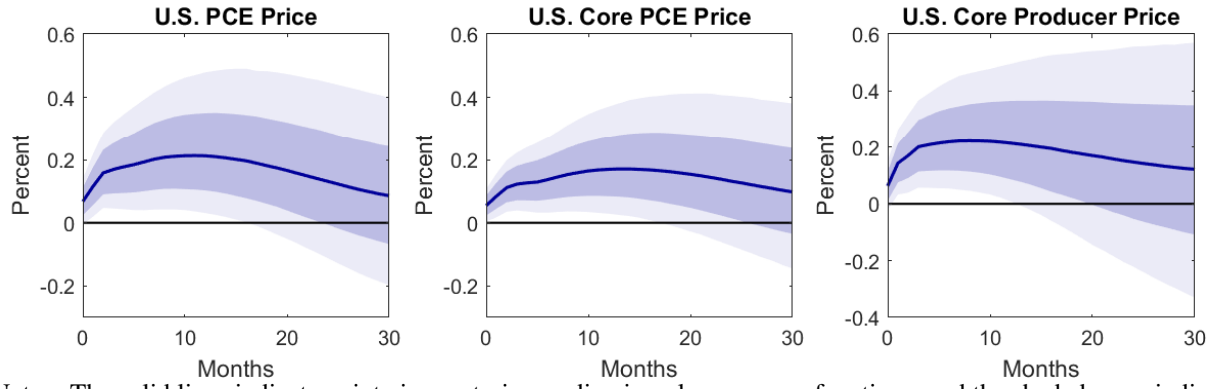
(a) Model with MCD-Container Index



(b) Lag Order $p = 12$



(c) Excluding the Strait of Hormuz Episode



Notes: The solid lines indicate pointwise posterior median impulse response functions, and the shaded areas indicate the 68% and 90% posterior credible sets. The IRFs are responses to an adverse two-standard-deviation shock to the MCD-Container index in panel (a) and to the MCD index in panels (b) and (c).

country i maximizes

$$\mathbb{E}_0 \sum_{t=0}^{\infty} \beta^t \left[U_i(C_{i,t}) - V_i(L_{i,t}^{\ell}) \right], \tag{3}$$

where $L^{\ell}_{i,t}$ denotes hours worked and $C_{i,t}$ is a CES aggregate of consumption of the goods produced in each country h, $C_{ih,t}$,

$$C_{i,t} = \left(\sum_{h=1}^{N} \left(\omega^{C}_{ih} \right)^{\frac{1}{\eta^{C}}} \left(C_{ih,t} \right)^{\frac{\eta^{C}-1}{\eta^{C}}} \right)^{\frac{\eta^{C}}{\eta^{C}-1}}, \tag{4}$$

with $\eta^{C} > 1$ governing the trade elasticity for final consumption goods and $\omega^{C}_{ih} > 0$ such that $\sum_{h=1}^{N} \omega^{C}_{ih} = 1$.[13]

International trade is subject to iceberg costs: delivering one unit of the good produced in h to country i for final consumption in period t requires shipping $\tau^{C}_{ih,t} > 1$ units, so a fraction $\tau^{C}_{ih,t} - 1$ is lost in transit. Trade costs are thus a technological feature of the model that determines the efficiency with which goods are moved across borders, and we model a shipping disruption as a decline in that efficiency. The logarithm of each bilateral trade cost follows an AR(1) process, $\ln \tau^{C}_{ih,t} = \rho_{\tau} \ln \tau^{C}_{ih,t-1} + \varepsilon^{C}_{ih,t}$, with $\varepsilon^{C}_{ih,t} \sim \mathcal{N}(0, \sigma^{2})$ for all i, h.

The law of one price holds. If $P_{h,t}$ is the price of the good produced in h in h's currency and $\mathcal{E}_{ih,t}$ is country i's nominal exchange rate against h, the price at the dock in i's currency is $P_{ih,t} \equiv \mathcal{E}_{ih,t} P_{h,t}$, and the price consumers in i pay, inclusive of trade costs, is $P^{C}_{ih,t} \equiv \tau^{C}_{ih,t} P_{ih,t}$.

Household ℓ maximizes (3) subject to the budget constraint

$$\sum_{h=1}^{N} \tau^{C}_{ih,t} P_{ih,t} C_{ih,t} + B_{ii,t} + \frac{B_{i1,t}}{\mathcal{E}_{1i,t}} \leq W^{\ell}_{i,t} L^{\ell}_{i,t} + R_{i,t-1} B_{ii,t-1} + R_{1,t-1} \Psi_{i,t-1} \frac{B_{i1,t-1}}{\mathcal{E}_{1i,t}} + T_{i,t} \tag{5}$$

for all t, where $B_{ii,t}$ denotes holdings of domestic bonds, $B_{i1,t}$ holdings of country 1's dollar-denominated bond, $W^{\ell}_{i,t}$ the household's nominal wage, and $T_{i,t}$ transfers.[14] The term $\Psi_{i,t-1}$ is a risk premium on the international bond that depends on the country's external borrowing, with $\Psi_{1,t} = 1$ and $\Psi_{i,t} \geq 1$ for $i \neq 1$.[15]

Expenditure minimization yields the demand for the good from each source country,

$$C_{ih,t} = \omega^{C}_{ih} \left(\frac{\tau^{C}_{ih,t} P_{ih,t}}{P^{C}_{i,t}} \right)^{-\eta^{C}} C_{i,t}, \tag{6}$$

[13] Complete financial markets within each country ensure that all households ℓ consume the same amount, so we omit the ℓ index in $C_{i,t}$.

[14] Transfers consist of firm profits. With tariffs, as in Cuba-Borda et al. (2025), they would also include tariff revenue rebated by the government.

[15] Appendix B.1 specifies the risk-premium function.

where

$$P^C_{i,t} \equiv \left(\sum_{h=1}^{N} \omega^C_{ih} \left(\tau^C_{ih,t} P_{ih,t} \right)^{1-\eta^C} \right)^{\frac{1}{1-\eta^C}} \tag{7}$$

is the consumer price index. We define the real exchange rate between i and h as $Q_{ih,t} \equiv \mathcal{E}_{ih,t} P^C_{h,t} / P^C_{i,t}$ and consumer (PCE) inflation as $\pi_{i,t} \equiv P^C_{i,t} / P^C_{i,t-1}$. Equations (5)–(7) make explicit that trade costs enter the prices consumers pay directly, so a shipping disruption affects consumption choices on impact, before any response of domestic prices.

Aggregate expenditure $C_{i,t}$ is determined by the Euler equation for domestic bonds. For countries other than country 1, whose households also hold the dollar bond, the optimal portfolio satisfies an uncovered interest parity (UIP) condition. Both conditions are derived in Appendix B.2.

Wage Setting. Nominal wages are sticky, as in Erceg et al. (2000). An employment agency (union) in each country combines households' hours into a homogeneous labor input $L_{i,t}$ through a CES aggregator with elasticity of substitution $\epsilon_w > 1$ and demands each household's labor so as to minimize its cost given the wages $W^\ell_{i,t}$; $W_{i,t}$ denotes the resulting aggregate wage index. Households set wages to maximize utility, but in each period a household can reset its nominal wage only with probability $1 - \theta_w$. The aggregate wage index therefore evolves according to $W^{1-\epsilon_w}_{i,t} = \theta_w (W_{i,t-1})^{1-\epsilon_w} + (1-\theta_w)(\overline{W}_{i,t})^{1-\epsilon_w}$, where $\overline{W}_{i,t}$ is the optimal reset wage. Appendix B.3 provides the derivations.

4.2 Firms

Each country has two types of firms. A unit continuum of differentiated firms, indexed by $v \in [0,1]$, produce nontradable goods using domestic labor and a bundle of intermediate inputs. A representative, perfectly competitive retail firm aggregates these differentiated goods into a homogeneous good that is traded internationally subject to trade costs. We describe each in turn.

4.2.1 Differentiated Firms

Firm v in country i produces according to

$$Y^v_{i,t} = A_{i,t} \left[(1-\nu)^{\frac{1}{\varepsilon_y}} L^v_{i,t}{}^{\frac{\varepsilon_y - 1}{\varepsilon_y}} + \nu^{\frac{1}{\varepsilon_y}} M^v_{i,t}{}^{\frac{\varepsilon_y - 1}{\varepsilon_y}} \right]^{\frac{\varepsilon_y}{\varepsilon_y - 1}}, \tag{8}$$

where $A_{i,t}$ is exogenous productivity, common to all firms in i, $L^v_{i,t}$ is labor, and $M^v_{i,t}$ is a bundle of intermediate inputs. The bundle is a CES aggregate of goods produced in all countries,

$$M_{i,t} = \left(\sum_{h=1}^{N} \left(\omega^M_{ih} \right)^{\frac{1}{\eta^M}} \left(M_{ih,t} \right)^{\frac{\eta^M - 1}{\eta^M}} \right)^{\frac{\eta^M}{\eta^M - 1}}, \tag{9}$$

where $M_{ih,t}$ denotes purchases by country i's firms of the good produced in h, $\eta^M > 0$ is the elasticity of substitution, and $\omega^M_{ih} > 0$ with $\sum_{h=1}^{N} \omega^M_{ih} = 1$. Firms face iceberg trade costs $\tau^M_{ih,t} \geq 1$ on imported inputs, whose logarithms follow AR(1) processes, $\ln \tau^M_{ih,t} = \rho_\tau \ln \tau^M_{ih,t-1} + \varepsilon^M_{ih,t}$ with $\varepsilon^M_{ih,t} \sim \mathcal{N}(0, \sigma^2)$, and a shipping disruption raises these costs as it does those on final goods. Because households and firms import the same good from a given country but face different trade costs, they pay different prices for it, which allows the model to match trade flows in final and intermediate goods separately.

Taking the prices of tradable goods $\{P_{h,t}\}_{h=1}^N$ as given, firms choose $M_{ih,t}$ to minimize the cost of the bundle, $\sum_{h=1}^{N} \tau^M_{ih,t} P_{ih,t} M_{ih,t}$, subject to (9). The resulting demands and the price index of the bundle, $P^M_{i,t}$, take the same form as (6) and (7) with M in place of C. Firms then choose labor and the bundle to minimize production costs, which yields the marginal cost

$$MC_{i,t} = \frac{1}{A_{i,t}} \left[(1 - \nu) W_{i,t}{}^{1-\varepsilon_y} + \nu (P^M_{i,t})^{1-\varepsilon_y} \right]^{\frac{1}{1-\varepsilon_y}}. \tag{10}$$

Trade costs on intermediate inputs enter marginal cost directly through $P^M_{i,t}$: a shipping disruption raises the price of the input bundle and hence firms' marginal costs. This is the channel through which disruptions generate persistent producer price inflation in Section 5.

4.2.2 Retail Firms

The representative retail firm in country i aggregates the differentiated goods available in i through a CES aggregator with elasticity of substitution $\epsilon > 0$ into a homogeneous good that can be consumed or used as an intermediate input, at home or abroad. Profit maximization yields the demand for each variety and the price of the homogeneous good in i's currency,

$$P_{i,t} = \left[\int_0^1 (P^v_{i,t})^{1-\epsilon} dv \right]^{\frac{1}{1-\epsilon}}, \tag{11}$$

where $P^v_{i,t}$ is the price set by firm v. This is the price at which the good produced in i is sold at the dock, so that, as in Section 4.1, $P_{hi,t} = \mathcal{E}_{hi,t} P_{i,t}$ is its price in country h before trade costs.

4.2.3 Price Setting

Differentiated firms set prices for their sales to retailers.[16] As with wages, a firm can reset its price in period t only with probability $1-\theta$. The price of the homogeneous good therefore follows $P_{i,t}^{1-\epsilon} = \theta P_{i,t-1}^{1-\epsilon} + (1-\theta)\overline{P}_{i,t}^{1-\epsilon}$, where $\overline{P}_{i,t}$ is the optimal reset price, derived in Appendix B.5.

4.3 Market Clearing and Balance of Payments

The tradable good produced in country i is consumed or used as an intermediate input at home and abroad, so market clearing requires

$$\xi_i Y_{i,t} = \sum_{h=1}^{N} \xi_h (\tau_{hi,t}^{C} C_{hi,t} + \tau_{hi,t}^{M} M_{hi,t}) \tag{12}$$

for $i = 1, \ldots, N$, where the population weights ξ_i appear because all variables are in per-capita terms. The trade costs on the right-hand side account for the goods lost in transit.

For every country $i \neq 1$, the balance of payments determines the evolution of holdings of the dollar bond,

$$B_{i1,t} - B_{i1,t-1} = \mathcal{E}_{1i,t}\left(EX_{i,t} - IM_{i,t}\right) + \left(R_{1,t-1}\Psi_{i,t-1} - 1\right) B_{i1,t-1}, \tag{13}$$

where $EX_{i,t} = P_{i,t}Y_{i,t} - P_{ii,t}C_{ii,t} - P_{ii,t}M_{ii,t}$ and $IM_{i,t} = \sum_{h\neq i} \tau_{ih,t}^{C} P_{ih,t} C_{ih,t} + \sum_{h\neq i} \tau_{ih,t}^{M} P_{ih,t} M_{ih,t}$ are exports and imports: the current account equals the trade balance plus net foreign investment income. Appendix B.6 provides the derivation.

4.4 Monetary Policy

The central bank in country i sets the nominal interest rate according to an inertial Taylor rule,

$$R_{i,t} = \left(R_{i,t-1}\right)^{\phi_i^r} \left(\frac{1}{\beta} \left(\pi_{i,t}\right)^{\phi_i^\pi} \left(\frac{GDP_{i,t}}{GDP_{i,t}^{flex}} \right)^{\phi_i^y} \varepsilon_{i,t}^{r} \right)^{1-\phi_i^r}, \tag{14}$$

where $GDP_{i,t}$ is real value added and $GDP_{i,t}^{flex}$ its level under flexible prices.[17] The parameter $\phi_i^r > 0$ governs interest rate inertia, $\phi_i^\pi > 0$ and $\phi_i^y > 0$ the responses to deviations of inflation

[16] Retail firms are perfectly competitive, so no firm sets prices in international markets. The setup is equivalent to producer currency pricing: prices are set in the producer's currency and foreign-currency prices move with the exchange rate.

[17] Real value added at steady-state relative prices is $GDP_{i,t} = \frac{P_i}{P_i^C} Y_{i,t} - \frac{P_i^M}{P_i^C} M_{i,t}$, where variables without a time subscript denote steady-state values.

from the zero target and of GDP from its flexible-price level, and $\varepsilon^r_{i,t}$ is a monetary policy shock. Country-specific rules allow us to compare the U.S. central bank's response to a disruption under alternative rules while holding the rest of the world's policy fixed, which is the exercise of Section 6.

5 Quantitative Analysis

We now turn to the model's quantitative predictions and ask whether it can reproduce the responses of U.S. prices and interest rates to a maritime chokepoint disruption estimated in Section 3. A positive answer is what justifies using the model in Section 6 to study specific episodes and alternative policy rules. We calibrate the model, construct a trade cost shock that matches the estimated response of freight rates, and compare the model's impulse responses with the SVAR estimates. The comparison is informative because the model is not calibrated to match the price and interest rate responses, only the size and persistence of the shock.

5.1 Calibration

Parameters. We follow Cuba-Borda et al. (2025) for all parameters except the persistence of trade cost shocks, which we set to match the dynamics of shipping costs estimated in Section 3. The world consists of five regions ($N = 5$): the United States, China, Asia excluding China, other advanced foreign economies (AFEs), and the rest of the world (ROW). As in Cuba-Borda et al. (2025), regions differ only in size, ξ_i, chosen to match their shares of world GDP, and in steady-state openness, governed by the bilateral preference parameters ω^Q_{ih} for $Q \in \{C, M\}$, chosen to match bilateral trade flows. Preferences allow for habit formation in consumption, with habit parameter $h \geq 0$ and inverse intertemporal elasticity of substitution $\sigma > 0$, and the disutility of labor is $V_i(L^\ell_{i,t}) = (L^\ell_{i,t})^{1+\varphi}/(1+\varphi)$, where $\varphi > 0$ is the inverse of the labor supply elasticity.

Table 1 reports the parameter values. Most are standard. The one that deserves comment is $\eta^Q = 5$ for $Q \in \{C, M\}$, which implies trade elasticities of $\eta^Q - 1 = 4$. These values are consistent with the long-run estimates of Simonovska and Waugh (2014), although Boehm et al. (2023) find lower elasticities at shorter horizons. We follow Cuba-Borda et al. (2025), who show that with these values the model captures the response of consumer prices to broadly defined trade cost shocks.

Shocks. Bilateral trade costs follow AR(1) processes with persistence ρ_τ. We choose ρ_τ and a configuration of trade cost shocks such that the model's average response of shipping costs matches the estimated response of freight rates in Figure 7, while preserving the rerouting of trade documented in Section 2.3.1. To do so, we raise each U.S. bilateral trade cost, $\tau^Q_{US,i}$ and $\tau^Q_{i,US}$ for $Q \in \{C, M\}$, in isolation and average the resulting responses across routes. Because trade can flow through the undisrupted routes, each disruption generates rerouting within the model, as in the data.

Table 1: Calibrated Parameters

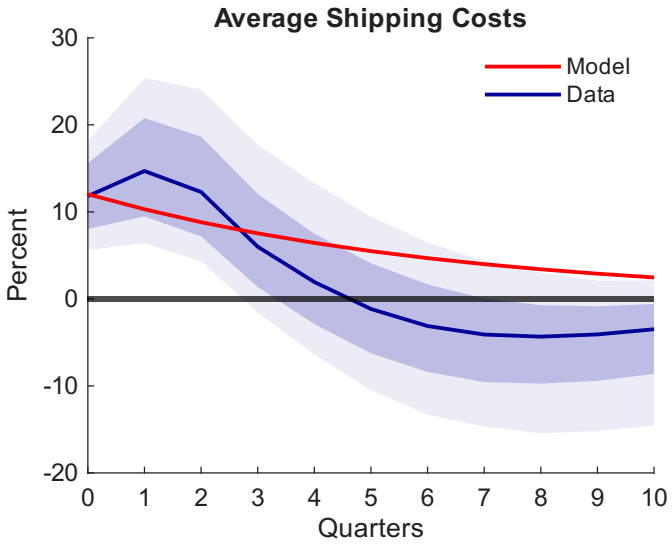
Parameter	Description	Value
Preferences		
β	Discount factor	0.99
σ	Inverse IES	0.5
h	Habit	0.75
φ	Inverse labor supply elasticity	2
η^C	Elasticity of substitution across source countries, final consumption	5
ϵ	Elasticity of substitution across differentiated goods	6
ϵ_w	Elasticity of substitution across labor varieties	6
Technology		
ν	Share of intermediates in production	0.4
ε_y	Elasticity of substitution between labor and intermediate inputs	0.5
η^M	Elasticity of substitution across source countries, intermediate inputs	5
Prices and wages		
θ	Price rigidity	0.8
θ_w	Wage rigidity	0.8
Monetary policy		
ϕ_π	Taylor rule inflation coefficient	1.5
ϕ_y	Taylor rule output coefficient	0.2
ϕ_r	Taylor rule inertia	0.75
ψ	Risk premium elasticity to NFA	0.001

We size each disruption as a 12 percent increase in trade costs, the increase that corresponds to a two-standard-deviation rise in the MCD index, scaled by one half to reflect the share of U.S. imports by value that arrive by water.[18] We also tilt the shock toward intermediate inputs by a factor of one half, holding the overall shock fixed, because imported capital goods and non-durable consumer goods are seldom bought directly by consumers (Campa and Goldberg, 2005).

Figure 9 compares the resulting path of average U.S. shipping costs in the model with the quarterly counterpart of the estimated response of the Drewry index in Figure 7. By construction, the shock matches the initial increase in shipping costs; thereafter the AR(1) process governs the dynamics. We use a one-time shock rather than a sequence of shocks that would track the estimated path more closely, because it isolates the dynamics generated by the model's mechanisms from

[18]The Bureau of Transportation Statistics reports $2.1 trillion in waterborne trade for 2023, of which imports made up 64.5 percent. That implies about $1.35 trillion in waterborne imports; compared with $3.084 trillion in total U.S. goods imports, the share is roughly 44 percent.

Figure 9: Shipping Costs: Model and Data



Notes: The solid red lines correspond to model-generated impulse responses. Blue lines indicate pointwise posterior median impulse response functions for the Drewry Composite Freight index, and the shaded areas indicate the 68% and 90% posterior credible sets. The IRFs are responses to an adverse two-standard-deviation shock to the maritime chokepoint disruption (MCD) index which in the model corresponds to a 12 percent increase in trade costs.

those generated by the path of the shock.[19]

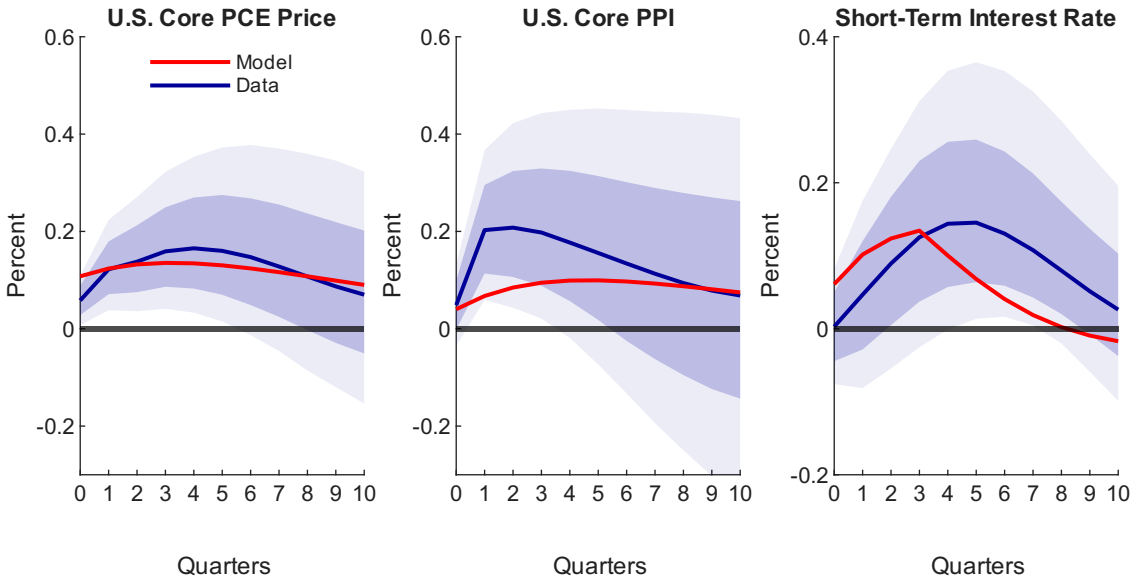
5.2 Responses of Prices and Interest Rates

Figure 10 compares the model's responses of U.S. consumer prices, $P^C_{US,t}$, producer prices, $P_{US,t}$, and the interest rate, $R_{US,t}$ (red lines), with the estimated responses of core PCE prices, core PPI, and the short-term interest rate (blue lines with 68% and 90% credible sets). The model matches the response of consumer prices closely (left panel). The impact response is slightly larger and the hump shape is somewhat less pronounced than in the data, but the model response stays near the median estimate and well inside the 90% credible set throughout.

Consumer prices reflect the prices of domestically produced goods and of imports. The middle panel shows the former, $P_{US,t}$, whose empirical counterpart is core PPI. The model reproduces the impact effect and the hump-shaped dynamics, and, as in the data, the hump is more pronounced for producer prices than for consumer prices.[20] The model generates a persistent rise in producer prices because firms import intermediate inputs and face nominal rigidities, so higher input costs are passed on gradually. The model falls short in one respect: it does not deliver the sharp rise in producer prices in the quarter after impact seen in the data. Two features of the exercise account

[19] An additional shock at quarter 1 would improve the fit to the estimated path but would also require recalibrating ρ_τ.
[20] As explained in Cuba-Borda et al. (2025), the direct effect of higher trade costs on the prices consumers pay for imports attenuates the hump in consumer prices relative to producer prices.

Figure 10: Responses of Prices and Interest Rate: Model and Data



Notes: The solid red lines correspond to model-generated impulse responses. Blue lines indicate pointwise posterior median impulse response functions, and the shaded areas indicate the 68% and 90% posterior credible sets. The IRFs are responses to an adverse two-standard-deviation shock to the maritime chokepoint disruption (MCD) index which we implement in the model as a 12 percent increase in trade costs.

for this. First, the one-time AR(1) shock omits the further increase in shipping costs observed in the data in the quarter after the shock (Figure 9). Second, price adjustment is time-dependent, so the share of firms that reset prices, $1 - \theta$, does not rise with the size of the shock. State-dependent pricing may deliver a larger response, as argued by Gilchrist et al. (2026), who show that the effects of higher shipping costs on U.S. PPI are consistent with predictions from a menu-cost model.

The right panel shows the interest rate responses. The model's path tracks the median estimate: the policy rate rises as inflation builds and falls as it recedes. The timing differs slightly: the model's rate jumps on impact and peaks after three quarters, whereas the estimated response rises with a lag and peaks after five quarters.

The model thus accounts for the joint dynamics of consumer prices, producer prices, and interest rates following a maritime chokepoint disruption. This is notable because our calibration does not target these responses. We next examine the responses of quantities, which our monthly SVAR does not include, both to characterize the macroeconomic effects of disruptions more fully and to expose the mechanisms at work.

5.3 Responses of Output, Trade, and the Exchange Rate

Figure 11 shows the responses of GDP, real marginal cost, the real exchange rate, imports, exports, and the trade balance to the same trade cost shock. The disruption acts as an adverse

supply shock. GDP falls by 0.4 percent after four quarters and remains 0.1 percent below steady state after ten quarters, by which time the increase in trade costs has almost fully dissipated. The mechanism is the rise in firms' real marginal cost, as shown in the upper middle panel: higher shipping costs raise the price of imported intermediate inputs, which lowers production efficiency and value added. Lower output and higher inflation together are the stagflationary response to trade cost shocks emphasized by Cuba-Borda et al. (2025).

The external adjustment is modest. Higher trade costs induce expenditure switching by consumers and firms toward domestically produced final and intermediate goods, which appreciates the dollar, but only by about 0.05 percent, because the disruption raises the cost of U.S. exports as well as imports and so dampens the effect of expenditure switching on relative prices. Gross trade flows, by contrast, respond strongly: imports and exports fall by about 11 and 13 percent on average over the first year, with the declines halving by the fourth quarter. The trade balance deteriorates by 0.15 to 0.2 percent of GDP over the first year, in line with the small appreciation. In sum, the model reproduces the estimated responses of prices and interest rates and delivers responses of output, trade, and the exchange rate that follow from its mechanisms and are consistent with evidence on related shocks.[21]

6 Episode Analysis and Policy Counterfactuals

We now use the model to study the two largest chokepoint disruptions in our sample: the Red Sea Crisis that began in late 2023 and the closure of the Strait of Hormuz in March 2026. The episodes differ in the size of the disruption and in the goods it affected, which makes them a useful pair for asking how the macroeconomic effects of a disruption, and the appropriate policy response, depend on its characteristics. For each episode, we calibrate the increase in trade costs to the rise in our disruption measure and trace the responses of prices, interest rates, output, and trade.

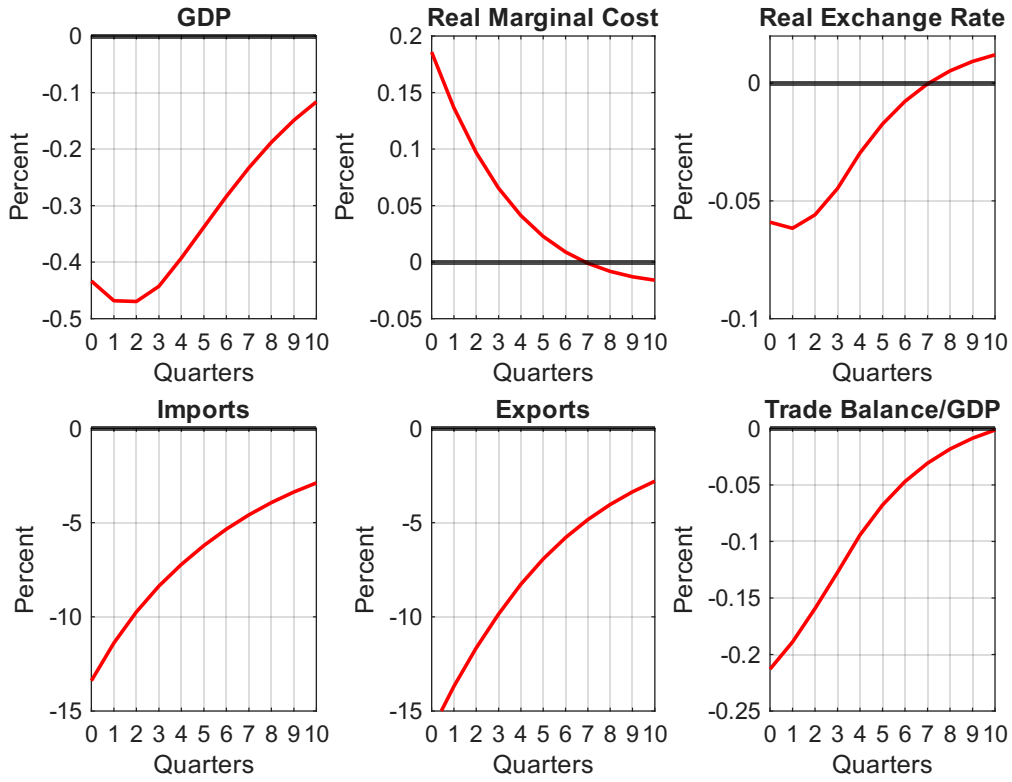
We compare outcomes under three monetary policy rules for the Federal Reserve. The first is the baseline Taylor rule in (14), which responds to consumer price inflation (PCE). The second responds to producer price inflation (PPI) instead,

$$R_{US,t} = R_{US,t-1}^{\phi^r_{US}} \left[\frac{1}{\beta} \left(\pi^{PPI}_{US,t} \right)^{\phi^\pi_{US}} \left(\frac{GDP_{US,t}}{GDP^{flex}_{US,t}} \right)^{\phi^y_{US}} \right]^{1-\phi^r_{US}} \varepsilon^r_{US,t}, \tag{15}$$

where $\pi^{PPI}_{US,t} \equiv P_{US,t}/P_{US,t-1}$. The case for targeting producer rather than consumer prices is that a disruption raises the prices of imported final goods directly, producing a one-time increase in

[21] The responses in Figure 11 are in line with the evidence in Cuba-Borda et al. (2025) for a large panel of countries following increases in broadly defined trade costs.

Figure 11: Responses of Other Macroeconomic Outcomes



Notes: The solid red lines correspond to model-generated impulse responses. The IRFs are responses to a 12 percent increase in trade costs.

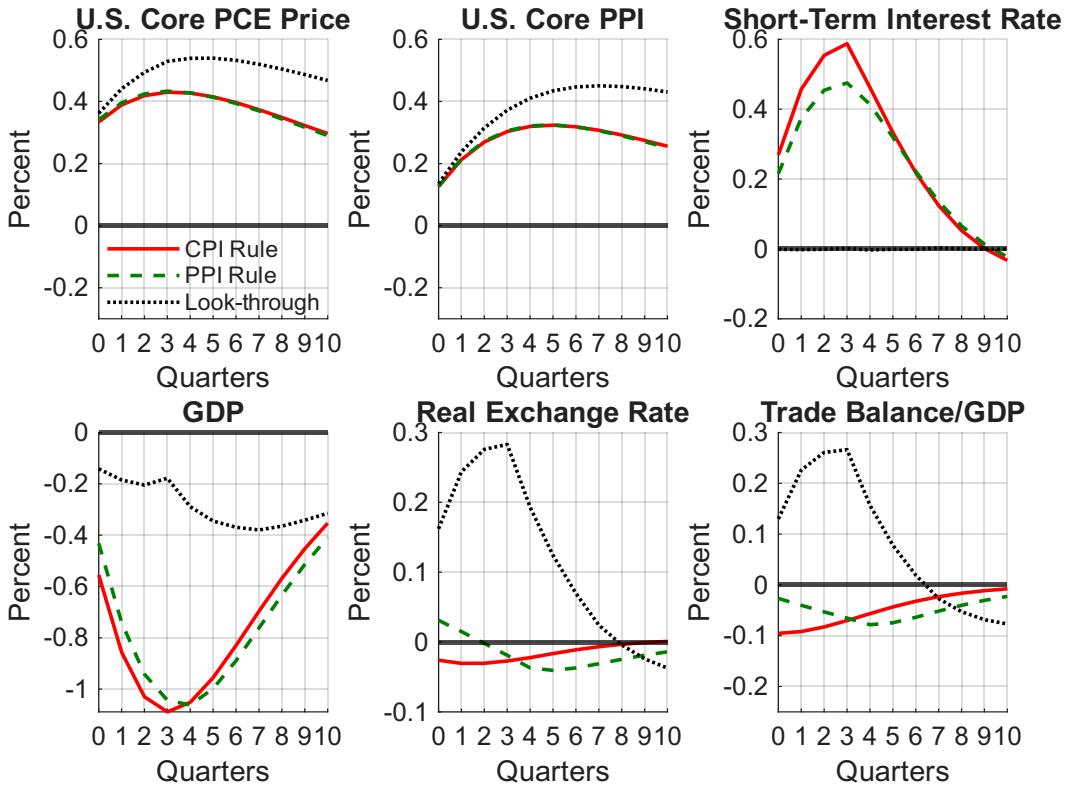
consumer prices that reflects a change in relative prices rather than in domestic inflationary pressure; a central bank that targets producer prices partially looks through this increase. The argument has been made for tariff shocks, which fall mainly on imported final goods (Bianchi and Coulibaly, 2025; Monacelli, 2025). Under the third rule, the central bank "looks through" the disruption entirely and holds the policy rate unchanged.[22]

6.1 The Red Sea Crisis

Calibration. We model the Red Sea Crisis as a 30 percent increase in route-specific shipping costs, the increase that corresponds to a five-standard-deviation rise in the MCD index (Figure 4). The shock has the same persistence as the average disruption in Section 5 and is allocated across final and intermediate goods in the same way. It is implemented as an increase in the cost of trading between the rest-of-the-world block, which includes the Middle East, and the other four regions. The disruption therefore hits every region that trades with the ROW, not only the U.S.,

[22] We implement this case through monetary policy shocks $\varepsilon^{r}_{US,t}$ in the baseline rule that offset the endogenous response of the policy rate.

Figure 12: Macroeconomic Effects of the Red Sea Crisis



Notes: Solid red lines: baseline consumer price (PCE) rule; dashed green lines: PPI rule; dashed black lines: look-through rule. The IRFs are responses to a 30 percent increase in trade costs, equivalent to a five-standard-deviation increase in the maritime chokepoint disruption (MCD) index.

which distinguishes it from the average U.S. disruption studied above.

Baseline. The solid red lines in Figure 12 show the responses under the baseline PCE rule. Consumer prices rise by almost 0.4 percent on impact, two and a half times the response to the average disruption, and peak three quarters after the shock, when four-quarter PCE inflation exceeds 0.4 percent. Producer prices follow a similar path but stay elevated for longer, peaking five quarters after the shock with four-quarter PPI inflation slightly above 0.3 percent. The greater persistence of producer prices, relative to the average disruption, reflects the global reach of the shock: because the price of intermediate inputs imported from the ROW rises for every region, firms worldwide raise prices as their marginal costs increase, and these higher prices feed back into marginal costs through imported inputs. The multi-region structure of the model is what allows us to capture this second-round effect.

In response, the U.S. central bank raises the policy rate by almost 0.6 percentage points relative to baseline. This response is consistent with the direction of policy at the time: when Houthi attacks in the Red Sea first forced ships to reroute around the Cape of Good Hope, FOMC participants cited

geopolitical disruptions to supply chains as an upside risk to inflation, and the rate cuts expected at the end of 2023 were delayed.[23]

On the real side (bottom row), GDP is about 1.1 percent below its pre-shock level one year after the disruption. The real exchange rate appreciates only marginally and the trade balance deteriorates slightly, both by less than after the average U.S. disruption, because a shock that raises trade costs for all regions trading with the ROW generates little expenditure switching toward or away from U.S. goods in particular.

PPI rule. How much of these effects reflects the U.S. central bank's response? Under the PPI rule, shown by the dashed green lines, the policy rate rises by less over the first six quarters, but the paths of consumer and producer prices are almost identical to those under the PCE rule. Two features of the model explain this. First, the disruption falls mostly on intermediate inputs rather than on goods consumers import directly, so PPI and PCE inflation move together and the two rules prescribe similar responses. Second, the Phillips curve in the model is flat, so the smaller output decline under the PPI rule does not translate into noticeably lower producer or consumer prices. The output difference is one of timing rather than size: the initial contraction in GDP is smaller under the PPI rule, but GDP stays depressed for longer. The shallower rate path also delays the exchange rate response, with the dollar appreciating gradually for five quarters before reverting, and the trade balance deteriorating by less initially and recovering after five quarters.

Look-through. The dashed black lines show the responses when the U.S. central bank holds the policy rate unchanged. Prices rise by more than under either Taylor rule: four-quarter PCE inflation exceeds 0.5 percent three quarters after the shock, and the price level remains more than 0.4 percent above its pre-shock level for two and a half years, driven mainly by producer prices. The output cost is much smaller on impact, with GDP falling only 0.2 percent after three quarters, but GDP then stays depressed through the end of the horizon, so that after two and a half years it is at about the same level as under the PCE rule. The fixed nominal rate and higher inflation lower the real return on U.S. bonds; demand for U.S. bonds falls, the dollar depreciates in real terms, and the trade balance improves.

Summary. The Red Sea Crisis added about 0.4 percentage point to U.S. core PCE inflation by the end of 2024 and led the central bank to tighten relative to its expected path, at a cost of about 1.1 percent of GDP. Targeting producer prices instead would have changed little, because

[23] The minutes of the January 30–31, 2024 FOMC meeting list "possible disruptions to supply chains from geopolitical developments" among the upside risks to inflation (https://www.federalreserve.gov/monetarypolicy/fomcminutes20240131.htm). The median projection for the federal funds rate at the end of 2024 in the Summary of Economic Projections rose from 4.6 percent in December 2023 (https://www.federalreserve.gov/monetarypolicy/fomcprojtabl20231213.htm) to 5.1 percent in June 2024 (https://www.federalreserve.gov/monetarypolicy/fomcprojtabl20240612.htm).

a disruption that works through imported inputs moves producer and consumer prices together. Looking through the disruption entirely would have raised the inflation cost to about 0.6 percentage point while limiting the initial output loss to 0.2 percent, at the price of a more persistent one.

6.2 The Closure of the Strait of Hormuz

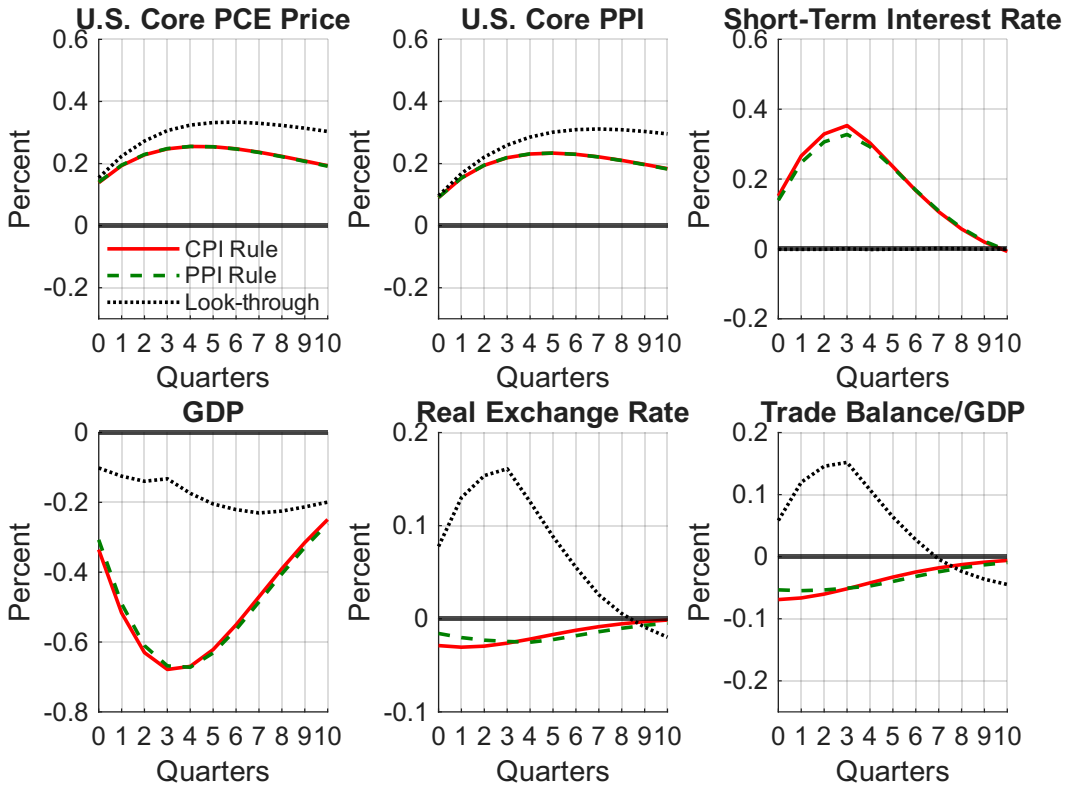
Calibration. The closure of the Strait of Hormuz in March 2026 differs from the Red Sea Crisis in two respects that matter for our analysis. First, the disruption to global shipping was smaller (Figure 4). Second, because the Gulf is the world's largest source of seaborne crude oil and refined products, the closure raised not only the cost of shipping goods but also the world price of energy. We study the first channel only. We calibrate the increase in trade costs to the rise in the MCD index. The model has no exogenous shock to the price of energy, so the exercise isolates the shipping channel from the energy price channel studied in recent work (e.g., Kilian et al., 2026).[24] Accordingly, we model the closure as an 18 percent increase in route-specific shipping costs, the increase that corresponds to a three-standard-deviation rise in the MCD index, with the same persistence and implementation as the Red Sea episode. Because trade through the Strait consists mainly of crude oil and refined products, which are intermediate inputs, we tilt the shock more heavily toward intermediate inputs than in the Red Sea episode.

Results. Figure 13 shows the responses under the three policy rules. The dynamics are qualitatively similar to those for the Red Sea Crisis, with smaller magnitudes. Under the baseline rule, consumer prices rise by less than 0.2 percent on impact, and the closure adds slightly more than 0.2 percentage points to four-quarter PCE inflation by the end of 2026. Almost all of the increase in consumer prices comes through producer prices, and the central bank raises the policy rate by slightly more than 0.3 percentage points after three quarters. GDP falls by 0.6-0.7 percent, and the responses of the real exchange rate and the trade balance are scaled-down versions of those in the Red Sea episode. The one qualitative difference is persistence: because the Hormuz shock falls more heavily on intermediate inputs, producer and consumer prices stay elevated for longer than after the Red Sea disruption.

The same feature governs the policy comparison. With the shock almost entirely on intermediate inputs, PPI and PCE inflation move together, and the responses under the PPI rule (dashed green) are nearly indistinguishable from those under the PCE rule. The look-through rule (dashed black) changes the dynamics as it did for the Red Sea Crisis: inflation is higher and the initial output loss smaller, so that the closure adds between 0.2 and 0.3 percentage points to four-quarter PCE inflation by the end of 2026, depending on the rule.

[24] The estimates in Kilian et al. (2026) capture any rise in shipping costs induced by higher fuel prices; ours capture the increase in trade costs from the physical closure in the absence of an exogenous energy price shock.

Figure 13: Macroeconomic Effects of the Closure of the Strait of Hormuz



Notes: Solid red lines: baseline consumer price (PCE) rule; dashed green lines: PPI rule; dashed black lines: look-through rule. The IRFs are responses to an 18 percent increase in trade costs, equivalent to a three-standard-deviation increase in the maritime chokepoint disruption (MCD) index.

Summary. The closure of the Strait of Hormuz added 0.2 to 0.3 percentage points to U.S. core PCE inflation through the shipping channel alone, depending on the monetary policy response, and its output cost is more sensitive to the policy rule than its inflation cost. These effects exclude the direct and second-round effects of higher energy prices, which would come on top of them.

7 Conclusion

Maritime chokepoints have become a recurring source of macroeconomic disturbance. When one of them closes, the consequences reach economies far from the disruption, and each closure raises the same questions for central banks: how large the effect on inflation is, how long it lasts, and whether to respond or look through it. These questions have been hard to answer because shipping disruptions are hard to separate from other shocks that accompany them. This paper answers these questions. We measure disruptions directly, from satellite tracking of vessel traffic through the world's major chokepoints, identify their causal effects from the exogenous events that trigger them, and interpret the estimates through a multi-country model with nominal rigidities in which disruptions raise the cost of trading goods across borders.

Our main finding is that maritime chokepoint disruptions are a supply shock in their own right. A disruption on the scale of a major chokepoint event raises U.S. consumer prices by about 0.2 percent for nearly two years, and most of that increase is in core prices. The shock travels along a chain we can observe at each link, from cargo volumes and freight rates to import, producer, and consumer prices, with the policy rate rising after a lag. The model reproduces these responses by recreating the average trade cost shock estimated in the data and identifies the mechanism: higher shipping costs raise the price of imported intermediate inputs and hence firms' marginal costs, which is why a disruption produces persistent inflation and lower output rather than a one-time jump in the price level.

Our results bear directly on monetary policy. In the model, the Red Sea Crisis raised U.S. consumer prices by about 0.4 percent on impact and kept inflation elevated for a year and a half, and the U.S. central bank raised the rate by 0.6 percentage points, consistent with the direction of policy at the time. A rule that targets producer rather than consumer price inflation would have changed little, because a disruption that enters through imported inputs moves producer and consumer prices together, so the PPI rule does not look through the shock. A central bank that looked through it entirely, holding the policy rate fixed, would have faced about 0.6 percentage point of additional inflation but a much smaller initial output loss. The closure of the Strait of Hormuz, through the shipping channel alone and setting aside its effect on energy prices, added at least 0.2 percentage points to consumer inflation by late 2026, and would have added more than 0.3 had the Federal Reserve looked through it. The broader lesson is that the trade-off a central bank faces after a chokepoint disruption depends on where the shock enters the economy. When it enters through intermediate inputs, as shipping disruptions do, there is no price index that lets policy look through it, and the choice is between tolerating higher inflation and accepting a larger output loss.

References

Arias, J. E., J. F. Rubio-Ramírez and D. F. Waggoner, "Inference Based on Structural Vector Autoregressions Identified by Sign and Zero Restrictions: Theory and Applications," *Econometrica* 86 (2018), 685–720.

Arslanalp, S., S. M. Choi, P. Kamali and J. Verschuur, "Nowcasting Global Trade from Space," IMF Working Paper WP/25/93, International Monetary Fund, May 2025.

Arslanalp, S., R. Koepke and J. Verschuur, "Tracking Trade from Space: An Application to Pacific Island Countries," IMF Working Paper WP/21/225, International Monetary Fund, August 2021.

Ascari, G., D. Bonam and A. Smadu, "Global Supply Chain Pressures, Inflation, and Implications for Monetary Policy," *Journal of International Money and Finance* 142 (2024), 103029.

Auclert, A., M. Rognlie and L. Straub, "The Macroeconomics of Tariff Shocks," Technical Report, National Bureau of Economic Research, 2025.

Auray, S., M. B. Devereux and A. Eyquem, "Trade Wars, Nominal Rigidities, and Monetary Policy," *Review of Economic Studies* 92 (2025), 2228–2270.

Bai, X., J. Fernández-Villaverde, Y. Li, R. Marto and F. Zanetti, "Shipping to America," NBER Working Paper 35808, National Bureau of Economic Research, September 2026a.

Bai, X., J. Fernández-Villaverde, Y. Li and F. Zanetti, "The Causal Effects of Global Supply Chain Disruptions on Macroeconomic Outcomes: Evidence and Theory," *forthcoming: American Economic Review* (2026b).

———, "State Dependence of Monetary Policy During Global Supply Chain Disruptions," Working Paper 35209, National Bureau of Economic Research, May 2026c.

Benden, P., "Global Shipping Lanes," Zenodo (2022), data set.

Benigno, G., J. di Giovanni, J. J. J. Groen and A. I. Noble, "The GSCPI: A New Barometer of Global Supply Chain Pressures," Staff Report 1017, Federal Reserve Bank of New York, May 2022.

Bergin, P. R. and G. Corsetti, "The Macroeconomic Stabilization of Tariff Shocks: What is the Optimal Monetary Response?," *Journal of International Economics* 143 (2023), 103758.

Bianchi, J. and L. Coulibaly, "The optimal monetary policy response to tariffs," Technical Report, National Bureau of Economic Research, 2025.

Bodenstein, M., P. Cuba-Borda, A. Queralto, R. Reyes-Heroles and I. Schott, "Optimal Monetary Policy under Higher Tariffs," Unpublished manuscript, 2026.

Boehm, C. E., A. A. Levchenko and N. Pandalai-Nayar, "The Long and Short (Run) of Trade Elasticities," *American Economic Review* 113 (2023), 861–905.

Burriel, P., I. Kataryniuk, C. Moreno Pérez and F. Viani, "A New Supply Bottlenecks Index Based on Newspaper Data," *International Journal of Central Banking* 20 (April 2024), 17–67.

Campa, J. M. and L. S. Goldberg, "Exchange Rate Pass-Through into Import Prices," *Review of Economics and Statistics* 87 (2005), 679–690.

Carrière-Swallow, Y., P. Deb, D. Furceri, D. Jiménez and J. D. Ostry, "Shipping Costs and Inflation," *Journal of International Money and Finance* 130 (2023), 102771.

Cerdeiro, D. A., A. Komaromi, Y. Liu and M. Saeed, "World Seaborne Trade in Real Time: A Proof of Concept for Building AIS-Based Nowcasts from Scratch," IMF Working Paper 2020/057, International Monetary Fund, 2020.

Chodorow-Reich, G. and J. Wieland, "Secular Labor Reallocation and Business Cycles," *Journal of Political Economy* 128 (2020), 2245–2287.

Christiano, L. J., M. Eichenbaum and C. L. Evans, "The Effects of Monetary Policy Shocks: Evidence from the Flow of Funds," *Review of Economics and Statistics* 78 (1996), 16–34.

———, "Monetary Policy Shocks: What Have We Learned and to What End?," in J. B. Taylor and M. Woodford, eds., *Handbook of Macroeconomics* (Elsevier, 1999), 65–148.

Comin, D. A., R. C. Johnson and C. J. Jones, "Supply Chain Constraints and Inflation," NBER Working Paper 31179, National Bureau of Economic Research, April 2023.

Cuba-Borda, P., A. Queralto, R. Reyes-Heroles and M. Scaramucci, "Trade Costs and Inflation Dynamics," Working paper, Federal Reserve Bank of Dallas, 2025.

di Giovanni, J., Ş. Kalemli-Özcan, A. Silva and M. A. Yildirim, "Global Supply Chain Pressures, International Trade, and Inflation," NBER Working Paper 30240, National Bureau of Economic Research, July 2022.

Dunn, J. and F. Leibovici, "Navigating the Waves of Global Shipping: Drivers and Aggregate Implications," Federal Reserve Bank of St. Louis Working Paper, 2023.

Erceg, C. J., D. W. Henderson and A. T. Levin, "Optimal Monetary Policy with Staggered Wage and Price Contracts," *Journal of Monetary Economics* 46 (2000), 281–313.

Finck, D., M. Klein and P. Tillmann, "The Inflationary Effects of Global Supply Chain Shocks: Evidence from Swedish Microdata," *European Economic Review* 189 (2026), 105426.

Finck, D. and P. Tillmann, "The Macroeconomic Effects of Global Supply Chain Disruptions," IMFS Working Paper 178, Institute for Monetary and Financial Stability (IMFS), Goethe University Frankfurt, 2023.

Forsythe, E., L. B. Kahn, F. Lange and D. G. Wiczer, "Where Have All the Workers Gone? Recalls, Retirements, and Reallocation in the COVID Recovery," *Labour Economics* 78 (2022), 102251.

Gertler, M. and P. Karadi, "Monetary Policy Surprises, Credit Costs, and Economic Activity," *American Economic Journal: Macroeconomics* 7 (2015), 44–76.

Gilchrist, S., B. Wei, V. Z. Yue and E. Zakrajšek, "Shipping Cost Shocks and US Producer Prices: Normal versus Crisis Pass-through," Policy Hub Paper 2026-7, Federal Reserve Bank of Atlanta, 2026.

Isaacson, M. and H. Rubinton, "Shipping Prices and Import Price Inflation," Federal Reserve Bank of St. Louis Review, 2023.

Kambourov, G., "Labour Market Regulations and the Sectoral Reallocation of Workers: The Case of Trade Reforms," *Review of Economic Studies* 76 (2009), 1321–1358.

Känzig, D. R. and R. Raghavan, "Supply Chain Shocks and the Macroeconomy: Evidence from Global Shipping Disruptions," Working paper, July 2026.

Kilian, L. and H. Lütkepohl, *Structural Vector Autoregressive Analysis*, Themes in Modern Econometrics (Cambridge: Cambridge University Press, 2017).

Kilian, L., M. D. Plante, A. W. Richter and X. Zhou, "The Impact of the 2026 Iran War on U.S. Inflation: A Scenario Analysis," Working Paper 2609, Federal Reserve Bank of Dallas, April 2026.

Kilian, L. and X. Zhou, "The Impact of Rising Oil Prices on U.S. Inflation and Inflation Expectations in 2020–23," *Energy Economics* 113 (2022a), 106228.

———, "Oil Prices, Gasoline Prices and Inflation Expectations," *Journal of Applied Econometrics* 37 (2022b), 867–881.

———, "Oil Price Shocks and Inflation," in G. Ascari and R. Trezzi, eds., *Research Handbook on Inflation* (Cheltenham, UK: Edward Elgar Publishing, 2025), 420–438.

Monacelli, T., "Tariffs and Monetary Policy," CEPR Discussion Papers 20142, Centre for Economic Policy Research, 2025.

Ramey, V. A., "Identifying Government Spending Shocks: It's All in the Timing," *Quarterly Journal of Economics* 126 (2011), 1–50.

Rubio-Ramírez, J. F., D. F. Waggoner and T. Zha, "Structural Vector Autoregressions: Theory of Identification and Algorithms for Inference," *Review of Economic Studies* 77 (2010), 665–696.

Schmitt-Grohé, S. and M. Uribe, "Tariff Staggering," Working Paper 35957, National Bureau of Economic Research, October 2026.

Simonovska, I. and M. E. Waugh, "The Elasticity of Trade: Estimates and Evidence," *Journal of International Economics* 92 (2014), 34–50.

UNCTAD, "Shipping Data: UNCTAD Releases New Seaborne Trade Statistics," (2025).

Werning, I., G. Lorenzoni and V. Guerrieri, "Tariffs as Cost-Push Shocks: Implications for Optimal Monetary Policy," Technical Report, National Bureau of Economic Research, 2025.

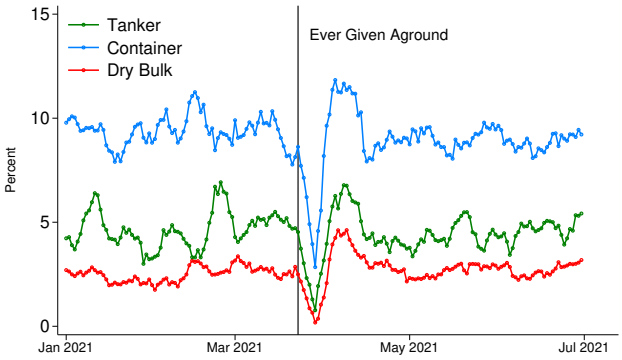
Online Appendix

A Additional Empirical Results

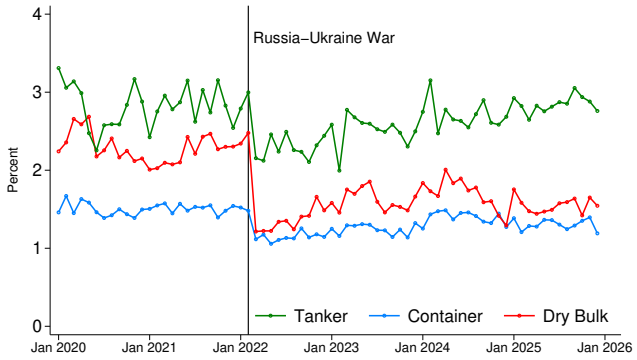
A.1 Additional Episodes of Maritime Chokepoint Disruptions

Figure A1: Transit Trade Volume Responses to Chokepoint Disruptions: Additional Episodes

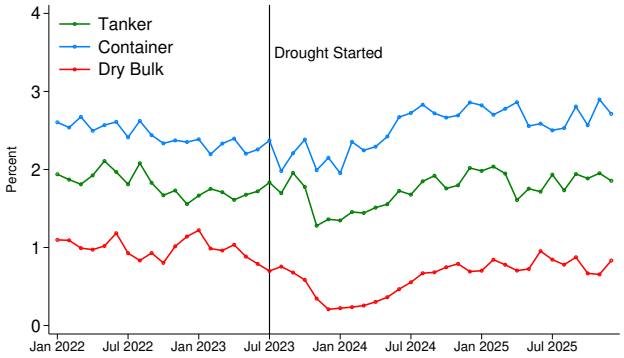
(a) Suez Canal



(b) Bosporus Strait



(c) Panama Canal

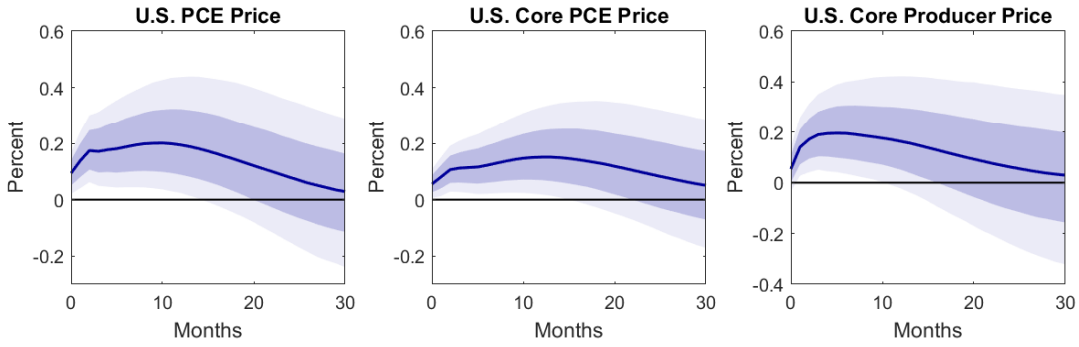


Source: IMF PortWatch Daily Chokepoint Transit Calls and Trade Volume Dataset. Notes: The figure shows transit trade volume through each chokepoint as a share of global shipping volume, by freight category. Trade volume data underlying panel (a) are seven-day moving averages, while data underlying panels (b) and (c) are monthly aggregates constructed from daily observations.

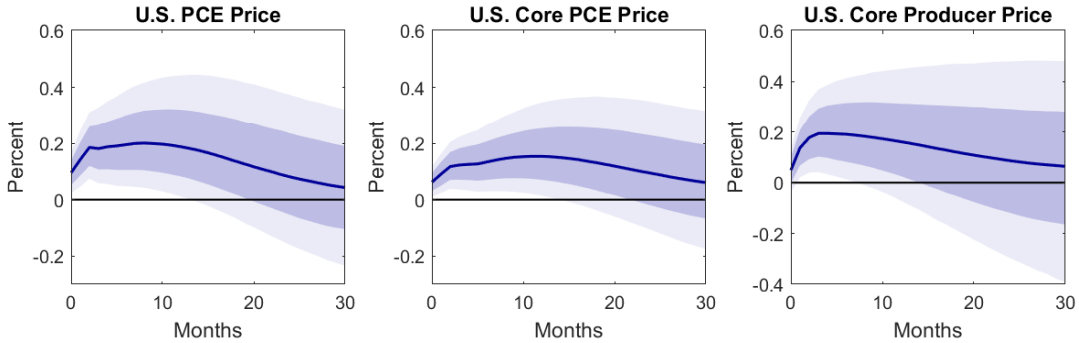
A.2 Additional Robustness Checks of SVAR Responses

Figure A2: Additional Robustness of U.S. Consumer and Producer Price Responses

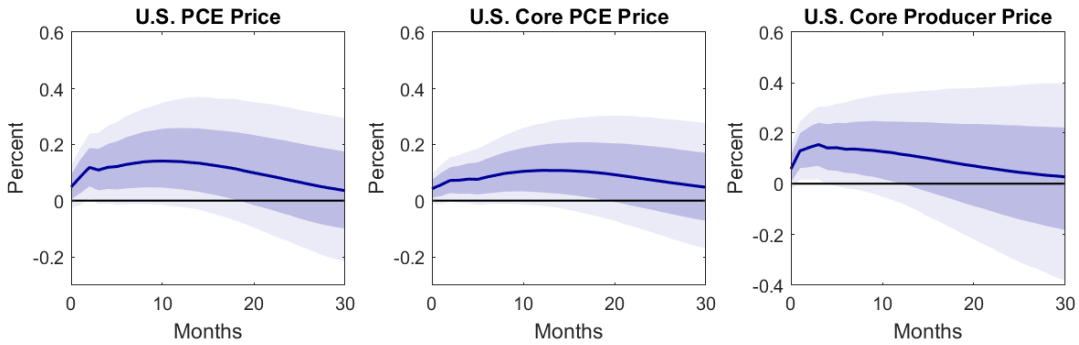
(a) Model with U.S. Retail Gasoline Prices



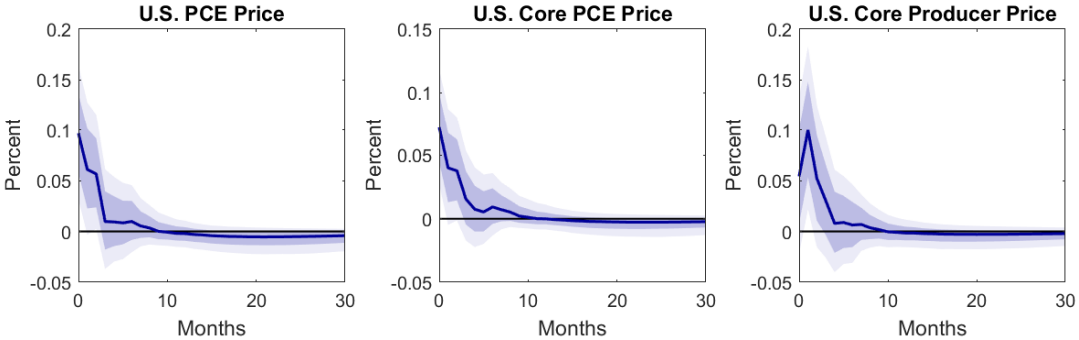
(b) Model with Treasury 3-Month Yield



(c) Excluding both Red Sea and Strait of Hormuz Episodes



(d) Growth-Rate Specification



Notes: The solid lines indicate pointwise posterior median impulse response functions, and the shaded areas indicate the 68% and 90% posterior credible sets. The IRFs are responses to an adverse two-standard-deviation shock to the maritime chokepoint disruption (MCD) index.

B Model Details

B.1 Households: Risk Premia

We assume that for $i \neq 1$, $\Psi_{i,t}$ is given by

$$\Psi_{i,t} \equiv (1 - \psi \frac{b_{i1,t}}{Q_{1i,t} Y_{i,t}}) \varepsilon_{i,t}^{\psi}, \tag{A1}$$

where $b_{i1,t} \equiv \frac{B_{i1,t}}{P_{1,t}^C}$ denotes country i's borrowing in units of country 1's good, $Y_{i,t}$ denotes total tradable output in country i, $\varepsilon_{i,t}^{\psi}$ is an exogenous shock to the risk premium of country i, and $Q_{ih,t}$ denotes the real exchange rate between country i and country h defined as

$$Q_{ih,t} \equiv \frac{\mathcal{E}_{ih,t} P_{h,t}^C}{P_{i,t}^C}, \tag{A2}$$

where $P_{i,t}^C$ is the ideal price index for final consumption, $C_{i,t}$, specified before.

B.2 Households: Euler Equation and UIP Condition

The Euler equation that characterizes the household's intertemporal optimality condition for bonds denominated in domestic currency is given by:

$$U_i'(C_{i,t}) = \beta R_{i,t} \mathbb{E}_t \left[\frac{U_i'(C_{i,t+1})}{\pi_{i,t+1}} \right], \tag{A3}$$

where $\pi_{i,t} \equiv \frac{P_{i,t}^C}{P_{i,t-1}^C}$ denotes CPI inflation.

For countries that trade bonds denominated in a currency other than their domestic currency, that is, for countries other than country 1, a household's optimal portfolio choice is characterized by an uncovered interest parity (UIP) condition, which in real terms is given by

$$R_{i,t} \mathbb{E}_t \left[\frac{U_i'(C_{i,t+1})/U_i'(C_{i,t})}{\pi_{i,t+1}} \right] = R_{1,t} \Psi_{i,t} \mathbb{E}_t \left[\frac{U_i'(C_{i,t+1})/U_i'(C_{i,t})}{\pi_{1,t+1} \frac{Q_{1i,t+1}}{Q_{1i,t}}} \right]. \tag{A4}$$

Hence, given our assumption about $\Psi_{i,t}$ in (A1), we have that the uncovered interest rate parity condition between countries i and 1 will not hold if $\frac{b_{i1,t}}{Q_{1i,t} Y_{i,t}}$ deviates from $\frac{1}{\psi}$.

B.3 Households: Wage Setting

The agency combines labor services across households according to

$$L_{i,t} = \left(\int_0^1 {L_{i,t}^{\ell}}^{\frac{\epsilon_w - 1}{\epsilon_w}} d\ell \right)^{\frac{\epsilon_w}{\epsilon_w - 1}}, \tag{A5}$$

where $\epsilon_w > 1$. Given a profile of wages across household types, $\{W_{i,t}^{\ell}\}_{\ell}$, the agency seeks to minimize its hiring costs by demanding labor services of type ℓ household according to

$$L_{i,t}^{\ell} = \left(\frac{W_{i,t}^{\ell}}{W_{i,t}} \right)^{-\epsilon_w} L_{i,t}, \tag{A6}$$

where

$$W_{i,t} = \left(\int_0^1 {W_{i,t}^{\ell}}^{1-\epsilon_w} d\ell \right)^{\frac{1}{1-\epsilon_w}}, \tag{A7}$$

and $W_{i,t}$ can be interpreted as the aggregate wage index in country i.

Households in each country compete in a monopolistic fashion in the labor market and therefore can set wages to maximize their utility. However, we assume that in any given period t, household ℓ can only reset its nominal wage, $W_{i,t}^{\ell}$, with probability $1 - \theta_w$, and that with probability θ_w, household ℓ's nominal wage has to be the same as in the previous period. Consider a household that can reset its nominal wage in period t. This household will choose its optimal reset nominal wage, $\overline{W}_{i,t}$, to maximize

$$\mathbb{E}_t \sum_{k=0}^{\infty} \beta^k \theta_w^k \left(U_i(C_{i,t}) - V_i(L_{i,t+k|t}^{\ell}) \right), \tag{A8}$$

where

$$L_{i,t+k|t}^{\ell} = \left(\frac{\overline{W}_{i,t}}{W_{i,t+k}} \right)^{-\epsilon_w} L_{i,t+k} \tag{A9}$$

denotes labor demand in period $t + k$ for a wage setter that last reset its wage in period t.

The optimal reset nominal wage has to be such that the following first order condition holds:

$$\mathbb{E}_t \sum_{k=0}^{\infty} \beta^k \theta_w^k L_{i,t+k|t}^{\ell} U_i'(C_{i,t+k}) \left(\frac{\overline{W}_{i,t}}{P_{i,t+k}^{C}} - \frac{\epsilon_w}{\epsilon_w - 1} \frac{V_i'(L_{i,t+k|t}^{\ell})}{U_i'(C_{i,t+k})} \right) = 0. \tag{A10}$$

Note that in the case in which workers can adjust wages in every period, $\theta_w^k = 0$, then we obtain the usual optimality condition that equates the real wage, $\overline{W}_{i,t}/P_{i,t}^C$, to the marginal rate of substitution, $V_i'(L_{i,t+k|t}^{\ell})/U_i'(C_{i,t+k})$, adjusted by the monopolistic distortion associated with a positive markup, $\epsilon_w/(\epsilon_w - 1)$. Since a measure θ_w of workers keep their wage unchanged and $1-\theta_w$ reset it optimally, the aggregate wage index, $W_{i,t}$, is such that $W_{i,t}^{1-\epsilon_w} = \theta_w (W_{i,t-1})^{1-\epsilon_w} + (1-\theta_w)(\overline{W}_{i,t})^{1-\epsilon_w}$.

B.4 Homogeneous Firms

To produce tradable goods, the representative retail firm in country i aggregates differentiated goods available in i according to

$$Y_{i,t} = \left(\int_0^1 Y_{i,t}^{v \frac{\epsilon-1}{\epsilon}} dv \right)^{\frac{\epsilon}{\epsilon-1}}, \tag{A11}$$

where $\epsilon > 0$. The output of the homogeneous good in country i can then be used for final consumption or as an intermediate input in the production of differentiated goods, either domestically or abroad.

Given the prices of different varieties, final good producers maximize profits subject to (A11). The solution to this maximization problem delivers the demand for variety v in country i:

$$Y_{i,t}^v = \left(\frac{P_{i,t}^v}{P_{i,t}} \right)^{-\epsilon} Y_{i,t}, \tag{A12}$$

where

$$P_{i,t} = \left[\int_0^1 (P_{i,t}^v)^{1-\epsilon} dv \right]^{\frac{1}{1-\epsilon}} \tag{A13}$$

defines the nominal price of a unit of the homogeneous good produced in country i in terms of its own currency, and $P_{i,t}^v$ denotes the nominal price charged by firm v in country i, also in terms of local currency units. As previously stated, excluding trade costs, the price of country i's imports from any country h is given by the price country h producers set domestically, adjusted for the exchange rate between the two countries, $P_{ih,t} = \mathcal{E}_{ih,t} P_{h,t}$.

B.5 Differentiated Firms: Price Setting

Let $\overline{P}_{i,t}$ denote the optimal price for a firm that is able to reset its price in period t. The firm sets this price to maximize

$$\mathbb{E}_t \sum_{k=0}^{\infty} \beta^k \theta^k \frac{U'_{i,t}(C_{i,t})}{P^C_{i,t+k}} \left(\overline{P}_{i,t} - MC_{i,t+k}\right) \left(\frac{\overline{P}_{i,t}}{P_{i,t+k}}\right)^{-\epsilon} Y_{i,t+k}, \tag{A14}$$

where the marginal cost is as specified in (10). The optimal price set by those firms able to adjust prices must be such that the following optimality condition holds:

$$\mathbb{E}_t \sum_{k=0}^{\infty} \beta^k \theta^k \frac{U'_{i,t}(C_{i,t})}{P^C_{i,t+j}} P^{\epsilon}_{i,t+k} Y_{i,t+k} \left[\overline{P}_{i,t} - \frac{\epsilon}{\epsilon - 1} MC_{i,t+k}\right] = 0. \tag{A15}$$

Note that under flexible prices ($\theta = 0$), this condition reduces to the usual pricing condition, setting prices equal to a markup over marginal cost. Since a measure θ of firms keep their price unchanged and $1 - \theta$ reset prices optimally, we obtain that $P_{i,t}$ follows $P^{1-\epsilon}_{i,t} = \theta P^{1-\epsilon}_{i,t-1} + (1-\theta)\overline{P}^{1-\epsilon}_{i,t}$.

B.6 Balance of Payments

To derive the balance of payments equation, we aggregate domestic budget constraints and obtain

$$\sum_{h=1}^{N} \tau^C_{ih,t} P_{ih,t} C_{ih,t} + \frac{B_{i1,t}}{\mathcal{E}_{1i,t}} = W_{i,t} L_{i,t} + R_{1,t-1} \Psi_{i,t-1} \frac{B_{i1,t-1}}{\mathcal{E}_{1i,t}} + T_{i,t}, \tag{A16}$$

where transfers to households in country i are given by firms profits, $T_{i,t} = \Pi_{i,t}$. Because profits are given by $\Pi_{i,t} = P_{i,t} Y_{i,t} - W_{i,t} L_{i,t} - \sum_{h=1}^{N} \tau^M_{ih,t} P_{ih,t} M_{ih,t}$, (A16) can be restated as

$$\sum_{h=1}^{N} \tau^C_{ih,t} P_{ih,t} C_{ih,t} + \frac{B_{i1,t}}{\mathcal{E}_{1i,t}} = P_{i,t} Y_{i,t} - \sum_{h=1}^{N} \tau^M_{ih,t} P_{ih,t} M_{ih,t} + R_{1,t-1} \Psi_{i,t-1} \frac{B_{i1,t-1}}{\mathcal{E}_{1i,t}}. \tag{A17}$$

Hence, we obtain that the evolution of holdings of U.S. bonds for country i—prescribed by the balance-of-payments condition—is given by

$$B_{i1,t} - B_{i1,t-1} = \mathcal{E}_{1i,t} \left(EX_{i,t} - IM_{i,t}\right) + \left(R_{1,t-1} \Psi_{i,t-1} - 1\right) B_{i1,t-1}, \tag{A18}$$

where $EX_{i,t} = P_{i,t} Y_{i,t} - P_{ii,t} C_{ii,t} - P_{ii,t} M_{ii,t}$ and $IM_{i,t} = \sum_{h \neq i} \tau^C_{ih,t} P_{ih,t} C_{ih,t} + \sum_{h \neq i} \tau^M_{ih,t} P_{ih,t} M_{ih,t}$ denote exports and imports. Condition (13) simply states that country i's current account is equal to its trade balance plus its net foreign investment income.